UNIVERSITY OF BELGRADE

FACULTY OF TECHNOLOGY AND METALLURGY

Omer Mohamed Yerro

SYNTHESIS AND CHARACTERIZATION OF FUNCTIONAL COMPOSITE MATERIALS FOR APPLICATIONS IN DENTISTRY

Doctoral Dissertation

Belgrade, 2016

UNIVERZITET U BEOGRADU

TEHNOLOŠKO-METALURŠKI FAKULTET

Omer Mohamed Yerro

SINTEZA I KARAKTERIZACIJA FUNKCIONALNIH KOMPOZITNIH MATERIJALA ZA PRIMENU U STOMATOLOGIJI

Doktorska Disertacija

Beograd, 2016

Supervisor

Dr Vesna Radojević, full professor, University Of Belgrade

Faculty of Technology and Metallurgy

Member of Committee

Dr Dušica Stojanović, Associate Research Professor, University Of Belgrade

Faculty of Technology and Metallurgy

Dr Petar Uskoković, full professor, University Of Belgrade

Faculty of Technology and Metallurgy

Dr Radmila Jančić-Hajneman, full professor, University Of Belgrade

Faculty of Technology and Metallurgy

Dr Mirjana Đukić, full professor, University Of Belgrade

Faculty of Pharmacy

Date:_____

ACKNOWLEDGEMENTS

It is a great pleasure for me to express my sincere gratitude to the people whose generous assistance and support this research.

I would like to take this opportunity to express my sincere thanks to my research advisor, Dr. Vesna Radojevic for all her guidance, direction and support during the evolvement of this thesis.

Special thanks to Dr. Dusica Stojanovic for her resourceful suggestions and technical support in experiments.

I would like to acknowledge Dr. Petar Uskokovic, Dr. Radmila Jancic-Heinemann and Dr. Mirjana Djukic my thesis examiners for their insightful suggestions and comments on my thesis.

SINTEZA I KARAKTERIZACIJA FUNKCIONALNIH KOMPOZITNIH MATERIJALA ZA PRIMENU U STOMATOLOGIJI

Rezime

Predmet ove doktorske disertacije obuhvata istraživanja u oblasti funkcionalnih kompozitnih materijala s polimernom matricom za primenu u stomatologiji. Ispitane su mogućnosti sinteze kompozitni materijala poboljšanih mehaničkih, termičkih i funkcionalnih svojstva. U okviru eksperimentalnog dela izvedena je sinteza i karakterizacija mikro do nanomodifikovanih dentalnih kompozitnih materijala na bazi autopolimerizujućih akrilata. Izvedeno je procesiranje funkcionalnih dentalnih kompozita ugradnjom nanoviskersa alumine, aktivnih agenasa za samozalečenje kao i čestica zeolita u polimernu matricu, kao i i njihova karakterizacija.

Za polimernu matricu predviđen je komercijalni dentalni poli(metil- metakrilat), Simgal, Galenika a.d. Procesiran je kompozit ugradnjom nanoviskersa aluminijum oksida-alumine čija je površina modifikovana u cilju ostvarivanja bolje veze sa polimernom matricom. Na taj način je dobijen kompoziti boljih mehaničkih i termičkih svojstava u odnosu na polaznu matricu. Kao modifikator površine nanoviskersa korišćen je 3-merkaptopropil-trimetoksi-silan i do sad, prema literaturi nije korišćen kod akrilatnih kompozita. Dodatak 3% m/m nanowiskersa alumine poboljšalo je termička svojstva kompozita, a jos veće povećanje je postignuto dodatkom modifikovanih nanoviskersa. Postignuto je značajno povećanje mehaničkih svojstava: metoda nanoindentacije je potvrdila povećanje redukovanog modula elastičnosti i tvrdoće za 65% i 90%, respektivno. Ispitivanje udarom kontrolisane energije pokazalo je da dodatkom nemodifikovanih nanoviskersa apsorbovana energija se smanjuje, dok se sa dodatkom modifikovanih nanoviskersa apsorbovana energija povećava značajno u odosu na čistu polimernu matricu. Ugradnjom agenasa za samozalečenje (diciklopentadiena u UF kapsulama i Grabs katalizatora prve generacije u PS vlaknima) regenerisana je apsorbovana energija za 74%.

Ispitana je i mogućnost ugradnje čestica zeolita 4A kao potencijalnih nosilaca funkcionalnih jona i molekula koji bi se ugrađivali u rešetku zeolita i koji bi daljim otpuštanjem funkcionalno poboljšali kompozit (npr. antimikrobni joni srebra kao i pojedini lekovi). Pokazano je da ugradnja čestica zeolita poboljšava mehanička svojstva akrilatne matrice. Uočeno je da sa porastom concentracije Zeolita raste i apsorbovana energija tokom udara.

U pravcu daljeg poboljšanja otpornosti na oštećenja, izvedeno je i procesiranje hibridnih komozita ugradnjom staklenih cevčica sa rastvorima aktivnih agenasa za samozalečenje (diciklopentadiena i Grabs katalizatora prve generacije). Postignuto je zalečenje od 83% apsorbovane energije.

Ključne reči: Kompozitni materijali, nanoviskersi, silanizacija, elektropredenje, nanoindentacija, ispitivanje udarom

Naučna oblast: Tehnološko inženjerstvo, Nauka o materijalima i inženjerstvo materijala

UDK: 66.017:616314

SYNTHESIS AND CHARACTERIZATION OF FUNCTIONAL COMPOSITE MATERIALS FOR APPLICATIONS IN DENTISTRY

Abstract

The aim of this dissertation was the research of functional composite materials with polymer matrix for use in dentistry. The posibility of synthesis of composites with improoved mevhanical, thermal properties and functionality was investigated. Synthesis and characterisation of nano to mikro modified dental composites on the basis of autopolymerized acrylates are performed.

As polymer matrix was used commercial dental autopolymerized acrylate Simgal, Galenika a.d. Serbia.First, the processing and characterization of acrylic resin reinforced with silanized alumina whiskers were performed. The nano whiskers of alumina have been functionalized by 3- mercaptopropyltrimethoxy silane (MPTMS) and embedded in auto polymerized acrylic resin. The content of whiskers was 3% w/w. The modification of the nano whiskers with the MPTMS silane enabled their dispersion and deagglomeration and yielded enhanced mechanical properties of the composite materials. As shown by nanoindentation tests, incorporation of 3 % w/w of silanized nano whiskers increased the reduced modulus and hardness of acrylic resin composite for 65% and 90%, respectively. The self-healing efficiency was demonstrated by impact test. A maximum healing efficiency of 74% is obtained for specimens containing 1 w/w % solvent microcapsules after 96 h of healing.

The posibility of embeding Zeolite 4A in acrylate also investigated. Zeolite is promising material as carrier of functional ions and molecules, i.e. antimicrobial silver ions or some medicine. The results indicate that the addition of Zeolite improved mechanical properties of acrylic resin. With the increasing content of Zeolite in the composite, impact the energy absorbed also increases.

This paper also presents a novel processing method of a self-healing acrylic thermoplastic material starting from a healing agent in solution form. The self-healing system consisted of a solution of the healing agent dicyclopentadiene (DCPD) in dimethylformamide (DMF) and a solution of the

catalyst bis(tricyclohexylphosphine) benzylidene ruthenium (IV) dichloride (called Grubbs' catalyst) in dichloromethane (DCM). Hollow glass tubes filled with the self-healing components were incorporated into autopolymerizing acrylic resins. The low energy impact tests of the samples showed a recovery of 83 % after 4 days.

Key words: acrylic composites, nanowiskers, silanization, electrospinning, nanoindentation, impact testing

Field of Academic Expertise: Technology engineering**,** Materials Science and Engineering

UDC: 66.017:616314

Content

THEORETICAL PART

Introduction

Composite material is a combination of two or more materials that results in better properties than those of the individual components used alone. This new material has completely unique, and totally new and different properties in relation to the contrasting individual components. Each material retains its separate chemical, physical, and mechanical properties. Composite as materials made from two or more constituent materials with significantly different physical or chemical properties, they can provide superior and unique characteristics different from their individual components. Similar to the long history of polymers, people made and used composite for many centuries. The earliest uses of composites can date back to the 1500s B.C. when early Egyptians and Mesopotamian settlers used a mixture of mud and straw to create strong and durable buildings. This is a good example for fiber reinforced composites which is the most common configuration for composite system. Again, with the development of synthetic polymers, particularly plastics, the modern era of composites begins. In the early 1900s, plastics such as vinyl, polystyrene, phenol and polyester were developed. Because plastics alone could not provide enough strength for structural applications, reinforcement was needed to provide the strength, and rigidity. The easy processing character provides the great potential as composite matrix materials for those polymers. In 1935, Owens Corning introduced the first glass fiber and later the glass fiber was used to reinforce plastic polymers as the pioneer work of the Fiber Reinforced Polymers (FRP) industry as we know it today. When combined with a plastic polymer, it creates an incredibly strong structure and also lightweight materials. Many of the greatest advancements in composites were incubated by war. Because the requirements in lightweight applications in military aircraft during the World War II, the FRP industry was brought into real production from laboratory and developed extremely fast. Also engineers realized other benefits of composites beyond being lightweight and strong at the same time. It was discovered that fiberglass composites were transparent to radio frequencies, and then the material was

utilized in sheltering electronic radar equipment. With time elapsed into the peaceful times, people began to try to fit composite into other markets to overcome the lower demand for military products. In the 1970s the composites industry began to mature. Better plastic resins and improved reinforcing fibers were developed. DuPont developed an aramid fiber known as Kevlar and also Carbon fiber was developed around this time. Those new fibers with improved properties bring more choice for the fiber reinforced composites. Beyond the traditional composites developed for structural applications, nowadays, the composite industry still rapidly growths with focusing on composites with various functions for renewable energy and other new applications and products. Corrosion chemical resistant composites are highly resistant to chemicals and will never rust or corrode. Boats made with fiberglass can stay in the highly corrosive salt water without rusting.

Composites with conductive particles dispersed in polymers can provide tunable conductivity and are widely used in industry as a type of conducting polymers. In the newest scientific studies, composites utilize even better fibers and resins and many of which incorporate nano-materials to provide nanocomposites.

The main advantages of composite materials are their high strength and stiffness, combined with low density [1]. A composite material consists of continuous phases where there is one or more discontinuous phase built in. The continuous phase is called the matrix or binder and the discontinuous phase is called an active filler or strengthener. The matrix surrounds and binds the groups of fibres or fragments of the reinforcement/support. The reinforcement/support, the active filler, provides a function of improving the mechanical properties and can also influence some other properties of the composite, such asthermal, electric, magnetic and optical. With the corresponding and correct choice of components and their relative mass molarity, one can get a material with the desired thickness, firmness, hardness, rigidity and resilience to corrosion and abrasion just like in high quality thermal or acoustic isolators.

The monophasic type phase, otherwise known as reinforcement, may be in the shape of a sphere (the particle), a cylinder (fibres, rods), laminated layer, irregular tiles (scales) or uneven/irregular particles (filler) all built into the continuous phase, i.e. the matrix. The reinforcements are typically strong and rigid materials, most commonly made of glass,

ceramics, metals or wood. The matrix is most often elastic and tough (for example, a polymer), although brittle matrices are used as well. The shape of the discontinuous (uneven/irregular) phase, contrasts and can be compared to a sphere (particle), a cylinder (fibres, rods), a laminated layer, irregular tiles (scales) or uneven/irregular particles (filler). The orientation of the discontinuous (irregular) phase can go in one, two or three directions, as shown in Figure 1. The composite is isotropic if the particles it contains are of different dimensions and are randomly orientated. If the particles are facing the same direction, then anisotropy is induced.
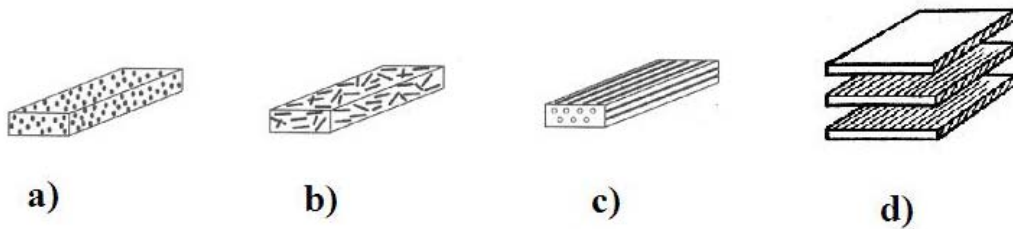
Figure 1. Shape of the reinforcements in composites: a) particle, b) short fibres ar wiskers, c) long fibers, d) laminate

Good characteriscis of composite materials in various industrial branches are: small mass, high strength relative to density, low sensitivity to abrasions, constructional adaptability, wear resistance, resistance to corrosion, dimensional stability, high compression resistance, high durability, small amount of energy used for production [2].

Classification of Composite Materials

There are a great number of composite materials and the largest number of composites is developed with the goal of improving their mechanical properties. First division is according origin to natural and synthetic composites. The second division of the

composite materials themselves can be made by looking at what type of reinforcements are used (figure 2.) [3], as well as the type of matrix (Figure 3.)

COMPOSITE MATERIALS

Synthetic

Natural

Layered   Cellular   Fibrous

Strengthened
by fibres

Strengthened
by particles

Constructional

Laminated

Sandwiched

Short fibres

Metal wire

Wiskers

Long fibres

Preferred
orientation

Random
orientation
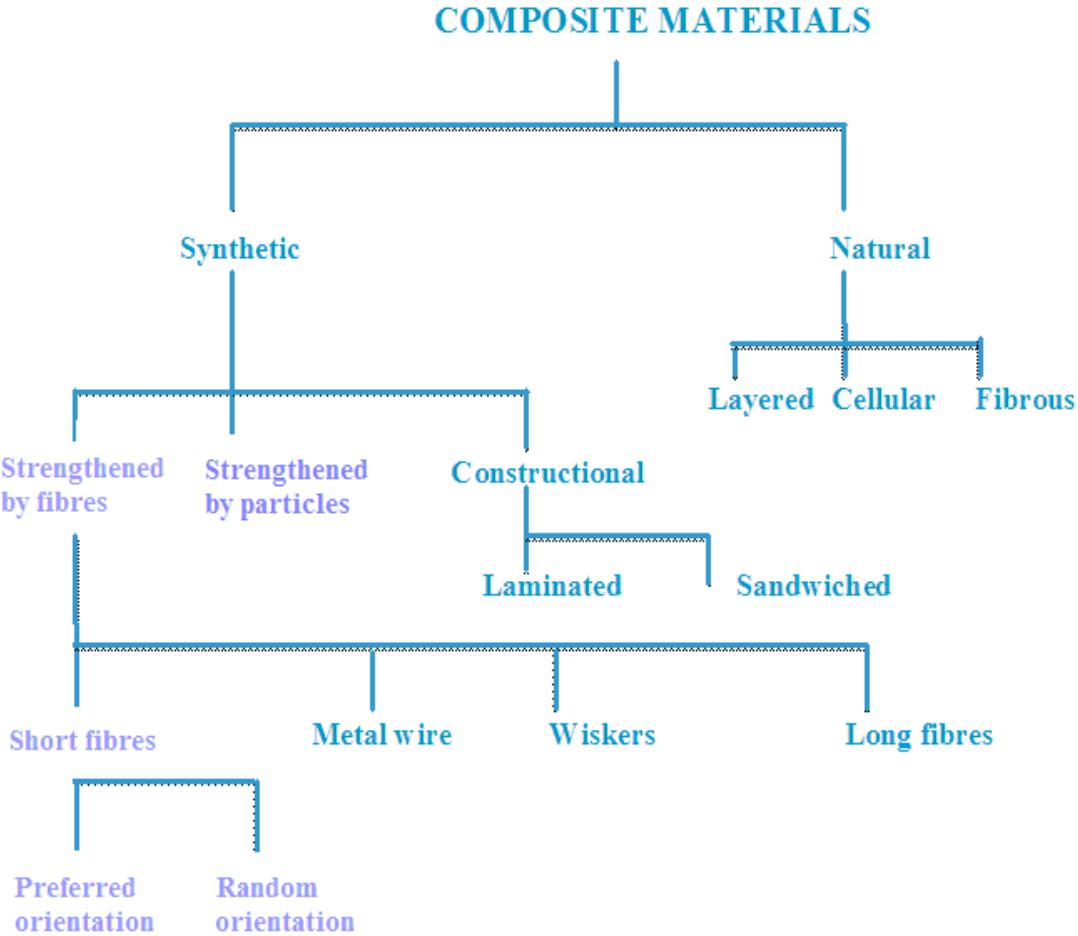
Figure 2. Classification of the composites by reinforcement shape

Depending on the matrix, the composite materials can be classified as synthetic composites (ceramic, polymer, carbon and metal) or as natural composites with a lignin matrix (wood) or collagen (bio composites), as shown in the following diagram (fig. 3) [4].
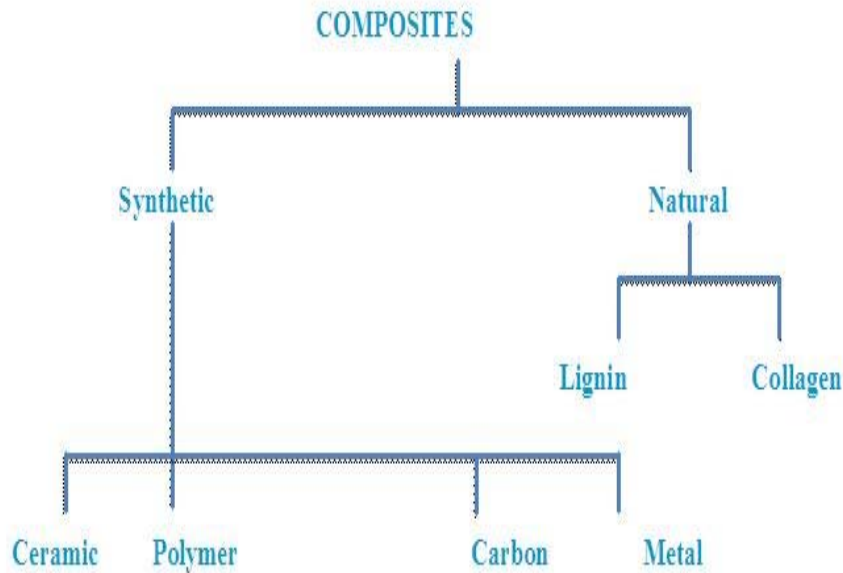
Figure 3. Classification of Composite Materials by Matrix Type

Types of Reinforcement in Composite Materials

In terms of reinforcement, composite materials can be divided into two groups:
-   Particulate composites (particle-reinforced composites)
-   Fibre reinforced composites and

Composites Reinforced With Particles

Particulate composites have dimensions that are approximately equal in all directions. They may be spherical, platelets, or any other regular or irregular geometry. Particulate composites tend to be much weaker and less stiff than continuous fiber composites, but they are usually much less expensive. Particulate reinforced composites usually contain less reinforcement (up to 40 to 50 volume percent) due to processing difficulties and brittleness.

Particulate composites are divided into composites reinforced by rough particles and composites reinforced by fine particles [5].

Rough particles are implied to be those with dimensions bigger than 1μm. In composites with rough particles the volume ratio of the dispersed phase (particle) is great. The most used composites in this group are: ceramic-metals, where the metal is the matrix, and the oxide of the non-metal/metal-polymer (matrix) and wood filler, which are dispersed in the plastic matrix.

The fine particles range from 10 nm to 100 nm. In the past decade there has been evidence of an expansion of the nanocomposites, or in other words, composites where the particle-reinforcement is about 1×10^{-9} m. Metals and their alloys are strenghtened by nano-particles of hard and inert materials. The most common reinforcement in polymer matrices are ones of inorganic origin, the first ones being titanium-dioxide, silicon-dioxide and aluminium silicate (clay), and where zeolites are also included. The interaction between the particles and matrices that leads to reinforcement happens on an atomic or molecular level. In this case the matrix carries the main part of the applied load, but small dispersed parts prevent and disturb the dislocation movement. Hence, the plastic deformation is limited so that the mechanical properties are improved.

Composites Reinforced By Fibres

One-dimensional fibres-like reinforcements of different thicknesses and direction could be added to the composite matrix. The strengthening fibres have to possess a high elastic modulus, high and uniform tensile strength, an acceptable thermal stability as well as given elastic behaviour under exertion/load.

The matrix has to fulfil functions of coalition/alignment of fibres and transfer of load onto them and protection of the strengthening fibres from chemical and mechanical effects .

Based on their geometric parameters, chemical nature and structure, the fibre strengtheners in the composites can be assorted into three different groups: whiskers, wires (metallic fibres) and fibres.

Whiskers are thin, nearly perfect, single-crystal fibres that have a large length/diameter ratio. Their extremely small size is overlooked by the fact that they have a high degree of crystallized perfection and are practically free of any flaws, which justifies their incredibly significant/large strength, and is the group made of the strongest recognised materials. Whiskers materials include graphite, silicon carbide, silicon nitride and aluminium oxide.

The wire is not very highly regarded as a composite component but the composites strengthened by it are very important. Typical wire strengtheners are usually made of steel, molybdenum and tungsten. Wires find applications as a radial steel reinforcement in automobile tyres, in filament wound rocket castings and in wire wound high-pressure hoses.

The fibers are the most important composites technologically. Design goals of fiber-reinforced composites often include high strength and/or stiffness on a weight basis. These characteristics are expressed in terms of specific strength and specific modulus parameters, which correspond, respectively, to the ratios of tensile strength to specific gravity and modulus of elasticity to specific gravity. Fiber-reinforced composites with exceptionally high specific strengths and modulus have been produced that utilize low-density fiber and matrix materials. Fiber reinforcements in composites could be in the form of short fibers (randomly or uniform oriented) or long or continuous fibers. A fiber has a length that is much greater than its diameter. The length-to-diameter (*l/d*) ratio is known as the *aspect ratio* and can vary greatly. Continuous fibers have long aspect ratios, while discontinuous fibers have short aspect ratios. Continuous-fiber composites normally have a preferred orientation, while discontinuous fibers generally have a random orientation.

Composite matrix

The composite matrix is required to fulfill several functions, most of which are vital to the performance of the material. Bundles of fibers are, in themselves, of little value to an engineer, and it is only the presence of a matrix or binder that enables us to make use of them. The roles of the matrix in fiber-reinforced and particulate composites are quite different. The binder for a particulate aggregate simply serves to retain the composite mass in a solid form, but the matrix in a fiber composite performs a variety of other functions

which must be appreciated in order to understand the true composite action which determines the mechanical behavior of a reinforced material [5]. The matrix binds the fibers together, holding them aligned in the important stressed directions. The matrix must also isolate the fibers from each other so that they can act as separate entities. The matrix should protect the reinforcing filaments from mechanical damage (*eg.* abrasion) and from environmental attack. A ductile matrix will provide a means of slowing down or stopping cracks that might have originated at broken fibers: conversely, a brittle matrix may depend upon the fibers to act as matrix crack stoppers. Through the quality of its 'grip' on the fibers (the interfacial bond strength), the matrix can also be an important means of increasing the toughness of the composite.

Metal-matrix composites

For **metal-matrix composites** (*MMC*s) the matrix is a ductile metal. The reinforcement may improve specific stiffness, specific strength, abrasion resistance, creep resistance, thermal conductivity, and dimensional stability. Some of the advantages of these materials over the polymer-matrix composites include higher operating temperatures, no flammability, and greater resistance to degradation by organic fluids. Metal-matrix composites are much more expensive than PMCs, and, therefore, their (MMC) use is somewhat restricted. The superalloys, as well as alloys of aluminum, magnesium, titanium, and copper, are employed as matrix materials. The reinforcement may be in the form of particulates, both continuous and discontinuous fibers, and whiskers; concentrations normally range between 10 and 60 vol. %. Continuous fiber materials include carbon, silicon carbide, boron, aluminum oxide, and the refractory metals. On the other hand, discontinuous reinforcements consist primarily of silicon carbide whiskers, chopped fibers of aluminum oxide and carbon, and particulates of silicon carbide and aluminum oxide [5].

Ceramic-matrix composites

In **Ceramic-matrix composites** (*CMC*s) is improved toughness of classic ceramic materials with particulates, fibers, or whiskers of one ceramic material that have been embedded into a matrix of another ceramic. This improvement in the fracture properties results from interactions between propagating cracks and dispersed phase particles. Crack initiation normally occurs with the matrix phase, whereas crack propagation is impeded or hindered by the particles, fibers, or whiskers. One particularly interesting and promising toughening technique employs a phase transformation to arrest the propagation of cracks and is aply termed *transformation toughening*. Small particles of partially stabilized zirconium are dispersed within the matrix material, often Al_2O_3 or ZrO_2 itself. Typically, CaO, MgO, Y_2O_3, and CeO are used as stabilizers [5].

Polymer Matrix Composites

Most commercially produced composites use a polymer matrix material often called a resin solution. There are many different polymers available depending upon the starting raw ingredients. There are several broad categories, each with numerous variations. The most common are known as polyester, vinyl ester, epoxy, phenol, polyimide, polyamide, polypropylene, polyether ether ketone (PEEK), and others. The reinforcement materials are often fibers but can also be common ground minerals [6]. The various methods described below have been developed to reduce the resin content of the final product. As a rule of thumb, hand layup results in a product containing 60% resin and 40% fiber, whereas vacuum infusion gives a final product with 40% resin and 60% fiber content. The strength of the product is greatly dependent on this ratio. PMCs are very popular due to their low cost and simple fabrication methods. Use of non reinforced polymers as structure materials is limited by low level of their mechanical properties, namely strength, modulus, and impact resistance. Reinforcement of polymers by strong fibrous network permits

fabrication of PMCs, which is characterized by the following: a) High specific strength b) High specific stiffness c) High fracture resistance d) Good abrasion resistance e) Good impact resistance f) Good corrosion resistance g) Good fatigue resistance h) Low cost [6].

Composites in dentistry

The introduction of resin-based dental materials around the mid of the last century was a revolution in restorative dentistry. Dental composites are esthetically pleasing since they possess tooth like appearance, are stable within the oral environment, are relatively easy to handle and do set on demand via LED or other blue light curing. Dental composites, however, still have several drawbacks. These include their polymerization shrinkage, potential failure of the resin–dentin interface leading to secondary caries, a relatively high coefficient of thermal expansion and a relatively low wear resistance compared to metal-based restorations. Leaching of uncured monomers from the composite may lead to cytotoxic effects in the surrounding gum tissues. Much of recent research on resin-based dental materials focused on these challenges and significant progress was made, although the basic principles of composition and effects of dental composites remained unchanged during the last decades. Beyond the recent improvements of dental composites, it is well worth to have a look at the potential future of this class of materials.. There are, however, a number of interesting developments and strong trends in the broader field of materials science and biomaterials, which may inspire future developments of dental composites to some extent. These developments include nanotechnology and nanostructuring, materials that actively fight microbes, stimuli responsive materials, materials that promote tissue regeneration or self-repairing materials.

The selection of a restorative material has significantly changed in recent years. Although dental amalgam is still considered a cost effective material, there is a growing demand for tooth colored alternatives that will provide the same clinical longevity that is enjoyed by dental amalgam. The use of composite resins has grown significantly internationally as a

material of choice for replacing amalgam as a restorative material for posterior restorations [7]. This demand is partially consumer driven by preference for esthetic materials and the concerns regarding the mercury content of amalgam [8]. It is also driven by dentists recognizing the promise of resin-based bonded materials in preserving and even supporting tooth structure. Numerous studies have suggested that bonding the restoration to the remaining tooth structure decreases fracture of multi-surface permanent molar restorations [9]. Modern composite resins have not yet achieved the level of mechanical properties found in dental amalgam. This has led to shorter clinical service and narrower clinical indications for composite resin materials compared to amalgam. Also, the polymeric denture base can consist of either a simple stiff base on which the teeth are arranged, or a sandwich of stiff base and a resilient liner to provide greater retention and comfort. So, this is also one exemplar of structure composite materials.

Primary constituents of the resin composite are:
- Resins
- Fillers,
- Coupling agent

Dental composite is composed of a resin matrix and filler materials. Coupling agents are used to improve adherence of resin to filler surfaces. Activation systems including heat, chemical and photochemical initiate polymerization. Plasticizers are solvents that contain catalysts for mixture into resin. Monomer, a single molecule, is joined together to form a polymer, a long chain of monomers. They need to be non reactive to the catalyst and resin.

There are now a wide range of materials used for filling and sealing teeth. Dental composite filler is generally applied to restore function and aesthetic appearance to a tooth. These types of composites are based on an acrylic monomer resin matrix, commonly PMMA, with a nano-to-micro-sized reinforcement. There are six main types of resin based composites [10].:

a) **Nano-to-Micro-filled Resin Based Composites-** The resulting material is ideal for anterior (front) teeth as it has low wear properties and excellent smoothness during application.

b) **Sealants**- Traditionally sealants were unfilled resins, but to increase their wear resistance manufacturers have added more filler. This increases the viscosity and reduces the ability of the sealant to flow into the defects within a tooth. Hence practitioners are moving towards flowable resin composites.

c) **Flowable Resin-based Composites-** Simply, this class of dental composite is a micro filled or hybrid resins with a reduced viscosity. The lower filler levels results in reduced strength and wear resistance.

d) **Packable Resin-based Composites-** Practitioners often have problems making good contact between the defect and the resin. This allows infections to get into the small cavity left between the filler and the defect and allows further tooth decay. Hence by packing a resin into the defect a better fit is achieved and no voids are left. The larger filler particle size of this type of composite has unknown wear characteristics and further research is in progress.

e) **Superficial Sealing filled Composites**- This material is an attempt at providing a complete resin restoration to a tooth. It is a combination of flowable resins with high wear resistance of a filled composite. This material requires a greater deal of preparation before it is applied to the tooth.

f) **Hybrid Resin-based Composites**- This resin is highly filled to obtain an optimum of mechanical properties (greater than micro filled resins) and an adequate aesthetic appearance. Hence, they are the most commonly applied composite in modern dental practice.

Polymer resins in dental composites

A Polymer is a large molecule or macromolecule, composed of many repeated subunits (monomers), which, by the process of polymerisation of many small molecules of covalent bonds, create a long chain. The repeating subunit, or monomer, is originally in a liquid state, however, through the process of polymerisation and its linkage leads to

increased mass viscosity resulting in the formation of a solid. Physical characteristics improve by combining more than one type of monomer and are referred to as a copolymer. Cross linking monomers join long chain polymers together along the chain and improve strength.

The organic polymer matrix in currently available composites is most commonly an aromatic or urethane diacrylate oligomer such as bisphenol A-glycidyl methacrylate (bis-GMA) or urethane-dimethacrylate (UDMA). The oligomers have in common reactive double bonds at each end of the molecule, which are able to undergo addition polymerization in the presence of free radicals. The oligomer molecules are highly viscous and require the addition of low-molecularweight diluent monomers, usually triethylene glycol dimethacrylate (TEGMA), so a clinically workable consistency may be maintained upon the incorporation of the filler.

Composite polymerization always involves a degree of shrinkage, depending on the organic matrix. Consequently, to reduce this negative effect, the dental industry has tested a great variety of monomers, including spiroorthocarbonates (SOCs), which expand, epoxy-polyol system combinations, which show 40%-50% less shrinkage in vitro than traditional systems, the siloxane-oxirane based resins or the use of high molecular weight molecules such as multiethylene glycol dimethacrylate and copolymers which manage to achieve 90%-100% conversion by reducing the C=C bonds. Ormocers (modified composites with organic and inorganic fillers) have also demonstrated their ability to reduce curing shrinkage, albeit minimally. Nonetheless, the main dental composite manufacturers currently still concentrate on the traditional systems, mostly adding a Bis-GMA/TEGDMA monomer or a Bis-GMA/UEDMA/TEGDMA combination to the organic matrix.

Acrylates used in creating the base in dentures, are commonly made by additional polymerisation of monomers, methyl-methacrylate (MMA), leading to the polymer polymethyl-methacrylate (PMMA). By activating the polymerisation method, the result is the affected by heat, chemical initiators, microwaves or light energy. On an everyday basis, heat-cured polymer and cold-cured polymer acrylates are used.
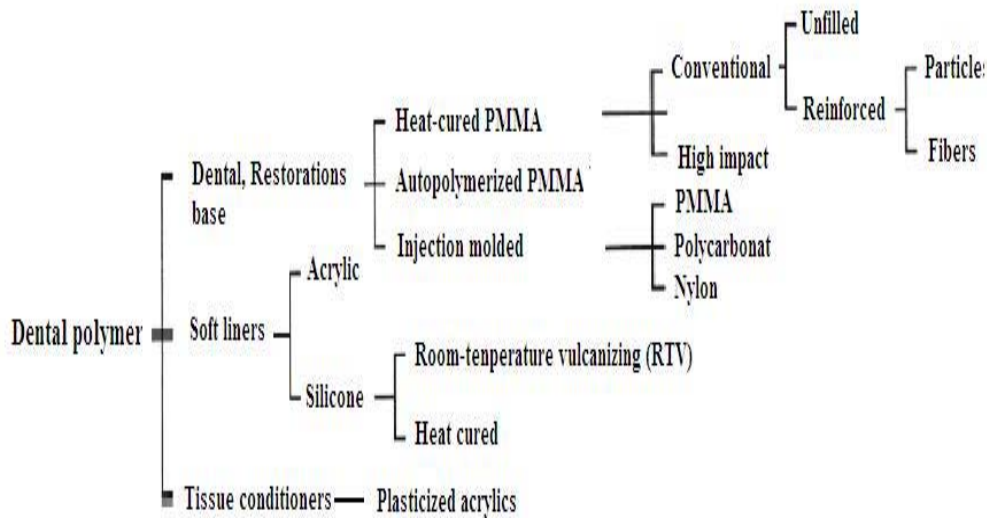
Figure 4. Classification of polymers in dentistry (after [5].)

Poly (methyl methacrylate) (PMMA) is one of the most important industrial polymers (Figure 5.). It could be produced by free radical polymerization of methyl methacrylate (MMA). Acrylic resins based on PMMA are used for the fabrication of various dental prostheses and denture liners, temporary crowns and orthodontic appliances [11-15]. In this work, an auto polymerizing acrylic resin was used as a thermoplastic matrix.
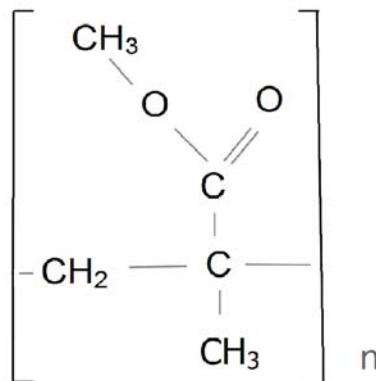
Figure 5. Structural Formula of PMMA [16]

The reason for their significant use is their appropriate physical and mechanical attributes, transparency, as well as their relatively easy manipulation/handling [17]. The use of this material is widespread because of its almost complete transition into a polymer, good adhesive properties with metals and porcelain, insolubility in the mouth cavity, good heat conduction, minor water absorption, natural appearance, translucency and biocompatibility. In everyday usage, heat-cured polymer and cold-cured polymer acrylates are used, which, according to their morphological and functional substituents in the mouth cavity, can be assorted into a biomaterial group [17-19]. It is also extremely chemically stable, not subject to oxidation as well as the effects of acids, alkalis and UV rays. Amorphous and can be processed to a large extent. The quality and durability depend on the amount of residual monomer in the polymerization reaction, ie the way in which the reaction is performed. Poor properties of poly (methyl methacrylate) are the brittleness and flammability. Due to its good properties, but also the relatively low prices, has widely applied in many industry segments, from engineering to the automotive industry, or as one of the most used materials in dentistry. PMMA as an ester of methacrylic acid belongs to the group of acrylic resin.

Poly (methyl methacrylate) is a synthetic polymer with transparency and resistance to atmospheric conditions combined with high strength and surface hardness. Because of that, it is often used as a substitute for glass. Its optical properties are remarkable, better than that of glass. Transparency is 92 % of light in the range of 380 to 780 nm [20]. PMMA polymerization reaction is performed with radical initiators in suspension or in mass. The reaction rate and the amount of newly formed polymer grow together with the degree of conversion. The initiator of the reaction is usually benzoyl peroxide.

The reinforcements and functional fillers in dental composites

Dental restorative composite materials with polymer matrix have found wide application due to their good mechanical properties, dimensional stability, aesthetics, simple processing and repairing capabilities. Typical materials that represent a good basis for strengthening is a acrylates that are often used for making dentures, as well as materials for relining and repair dentures. The reinforcement in the form of inorganic particles improves the physical and mechanical properties of dental restorative composites.

Resin composites are generally composed of modified particulate fillers in a polymeric matrix derived from the polymerization of a mixture of methacrylate monomers. Inorganic fillers provide strength, wear resistance, and translucency in addition to reducing the overall shrinkage of the composites. Commonly used reinforcements are glass, quartz, colloidal silica, silica nanoparticles, and zirconia-silica nanoclusters. Barium or strontium containing glasses, or zirconia particles, are often added to provide radiopacity and contrast needed for the clinical diagnosis of marginal leakage and secondary caries in resin based restorations120]. Hydroxyapatite is a natural component of enamel and dentin and hence it has been considered as a filler material for resin composites. Hydroxyapatite is naturally radiopaque and moisture resistant. However, it was shown that porosity and filler particle aggregation lead to increased water uptake and solubility of the base resin [22], limiting their applicability as a filler.

Besides ceramic particles [4], chopped glass fibers and porous networks of fibers have also been incorporated as fillers into dental composites and bone cements [23, 24]. The advanced composite research is focused on producing a material that has perfect filler–resin interface and improvement in filler packing, optimization in filler levels, and development of hybrid filler phases [25, 26]. The transition to nanocomposites yields dramatic changes in physical properties. Nanoscale materials have a large surface area for a given volume. These fillers are classified by their geometries as: particle, fibrous, and layered. Fibrous materials provide reinforcing efficiency because of their high aspect ratios and single crystal nanowhiskers are close to that definition. The ceramic whiskers are single crystals possessing a high degree of structural perfection and, hence, superior strength and

toughness values. So, they were described as reinforcement in a polymer composite [27, 28].

Filler content, filler size, and distribution of filler play important roles in governing the physical and mechanical properties of resin composites [29]. Higher filler content and coarser size are usually associated with improved mechanical properties such as strength and modulus, but smaller particle size, which leads to enhanced volume fractions, provide higher wear resistance and aesthetic properties [22- 31].

Alumina and alumina/silica compounds

Some studies have evaluated silica-glass fibers as reinforcing filler materials [32]. Although fiber reinforced composites have higher strength, toughness, and fatigue resistance, difficulties accommodating higher fiber content, insufficient fiber wetting, difficulty in manipulating free fibers, and rough surface characteristics [33] have restricted their widespread usage in dentistry [34]. Recently, silicon carbide and silicon nitride whiskers have also been tried as fillers with the purpose of enhancing the strength and toughness [35] of the composites. The nano particles and hence nanowhiskers behaved as functional physical crosslink and thus reduced the overall mobility of the polymer chains, leading to better thermal and mechanical properties. Alumina nanowiskers have good potentials for improvement of thermal and mechanical properties [36-39], and also posses a good osteoblast (bone-forming cell) function [40].
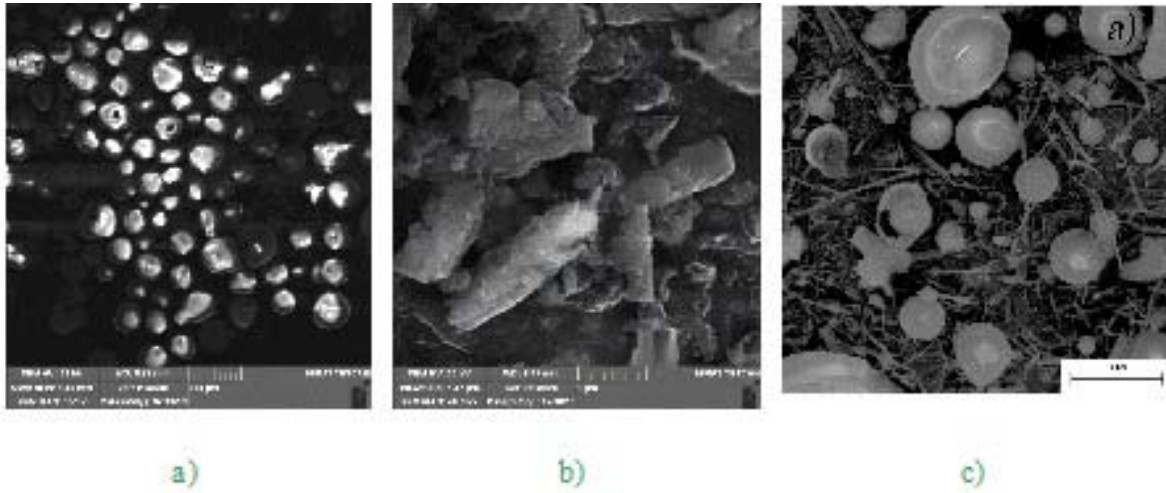
Figure 6. Different shape of alumina fillers in dental composites: a) particles; b) whiskers; c) fibers [37, 38]

The earliest work involving Al_2O_3 as reinforcement for composite materials concerned the use of tiny filamentary crystals, of the order of 50μm long and a few microns in diameter-whiskers, which could be grown from the vapor phase in a highly perfect state and which, in consequence, had great strength and stiffness [40]. The DuPont Company in the USA subsequently developed an improved alumina fiber in the form of a polycrystalline yarn known as FP fibre (Dhingra, 1980). These filaments, which were manufactured by a sol-gel process, had a modulus comparable with those of boron and carbon, and strength of the order of 1.8GPa. Wallenberger and Brown (1994) [41] have given a useful graphical plot, drawn in modified form in Figure 7, showing how the tensile stiffness of this particular family of materials varies with composition.
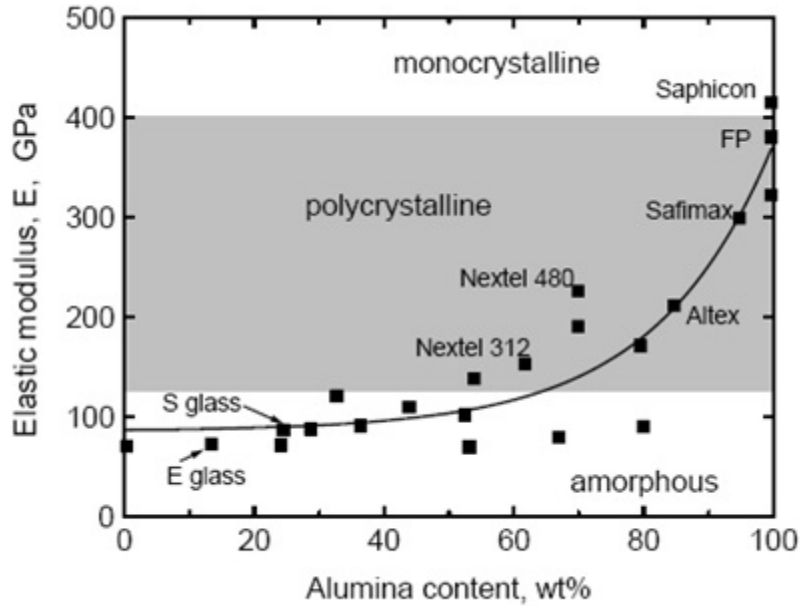
Figure 7. Modulus of elasticity of silica/alumina fibers labelled with their familiar trade names [41]

Functional fillers in dental composites

Some filler in dental composites have no role for mechanical reinforcements of composite, but there have some other functions: thermal, optical, drug delivery, antimicrobial properties and self healing [42-51].

A new quality of dental composites may, however, be created if nanotechnology is used and other new developments in material science and biomaterials are considered in composites in the future. Currently, the particle sizes of conventional composites are so different from the structural sizes of hydroxyapatite crystals, dental tubules, and enamel rods, compromises in adhesion between the macroscopic (40-0.7 nm) restorative material and the nanoscopic (1-10 nm in size) tooth structure are potential. Nanotechnology can, however, improve this continuity between the tooth structure and the nanosized filler

particle and provide a more stable and natural interface between the mineralized hard tissues of the tooth and these advanced restorative biomaterials [42, 43]

Silver and titanium particles were introduced into dental composites, respectively, to introduce antimicrobial properties and enhance the biocompatibility of the composites [43, 44].

This paper relates to self-polymerizing methyl methacrylate (PMMA) and more particularly to restorative materials having self-healing characteristics, or the capability to autonomously heal the cracks occurring in the material. Tensile loading, fatigue loading, impact damage and thermal cycling can result in the formation of micro cracks in composite materials, which can result in a drastic reduction in mechanical properties. The study of self-healing materials is biologically inspired where damage initiates a self-directed healing response of smart and self-healing materials.

Antimicrobial materials fight bacteria and delay, reduce or avoid the formation of biofilms on the materials. There are dif ferent strategies to accomplish this. Generally, antimicrobial properties of (bio) materials may be accomplished by introducing agents such as sliver or one or more antibiotics into the material. Microbes are subsequently killed on contact with the materials or through leaching of the antimicrobial agents into the body environment. There are several examples of antimicrobial biomaterials used as implants or in pure research and the number of studies, addressing antimicrobial biomaterials outside the field of dental materials has recently increased rapidly. In the oral cavity, important examples of microbes present are acid producing bacteria, such as Streptococcus mutans or anaerobic bacteria. A common problem with composites is the failure of the resin dentin interface, although new and improved bonding systems have helped to reduce the problem. If the interface fails, bacteria as mentioned above are able to penetrate the gap, which may result in secondary caries. Therefore, a need exists to have dental composites with antimicrobial properties.

Zeolites

Zeolites are microporous, aluminosilicate minerals, elements in the first and second group of the periodic table (sodium, potassium, magnesium and calcium). There are now recognised, more than 150 synthetic and 40 zeolites that are in nature. Structurally, zeolites are aluminosilicate minerals made from interlinked tetrahedra of alumina (AlO_4) and silica (SiO_4). Zeolites can be represented with the empirical formula:

$$M_{2/n}O \cdot Al_2O_3 \cdot xSi \cdot yH_2O$$
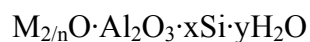
In this formula, x is generally greater or equal to 2 because in AlO_4, the tetrahedra are joined to SiO_4 tetrahedra and n is the valency cation. Zeolites have a porous structure that can accommodate a wide variety of cations, such as Na^+, K^+, Ca^{2+}, Mg^{2+} and others, including water molecules. These positive ions are rather loosely held and can readily be exchanged for others in a contact solution. It is these connected channels and pores that give it its specific properties. The size of these pores is usually the size of molecules between 3 to 10 x 10^{-10} m.

Aluminium atoms are trivalent, which is why there is an abundance of negative electric charge in the lattice when the Si atom replaces the Al in the tetrahedron. This charge is compensated by cations that are not in the structure, but are close by, most often being the cations Na^+, K^+, i Ca^{++}. The number of cations determined by the number of aluminium atoms in the network/lattice. Due to the presence of cations, zeolites are polar absorbers. This means that the polar compound molecules such as water, ammonia, carbon dioxide, nitrogen and aromatic hydrocarbons will be more easily absorbed than nonpolar molecules of the same size. Molecules with a high silicon/aluminium ratio are hydrophobic and absorption is mostly done through Van der Waals's force.

Four major factors influence absorption properties of zeolites:

1. Size of the pore that influences the ability of the molecule to enter and diffuse through the zeolite's lattice.
2. The silicon/aluminium ratio, which determines the number of cations and hydrophility of the zeolite lattice/network.

3. Type of cation (valency and size)
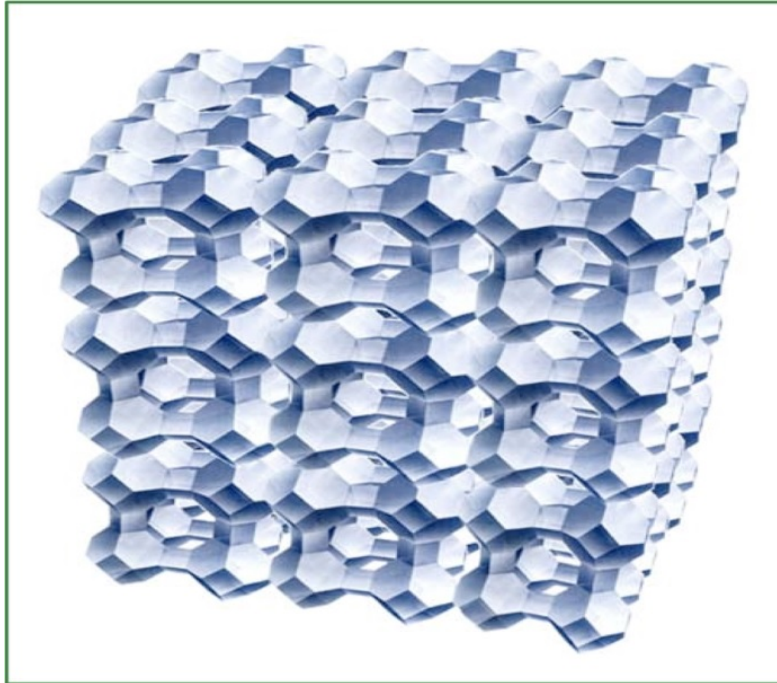4. Direction of the pores within their space.

Figure 8. Zeolite network structure

Zeolites are known for their incredibly thermic and chemical stability and are most often used in the form of particles as catalysts, detergents and in ion-exchange and separation of gases. This multi-use, non-toxic and cheap material is also used for hygienic purposes such as odour repellents, as well as for medical uses. All of these properties are formed on a uniform micro- (even nano-) porous level of zeolites (3-13A), which allows for the sifting of the molecule.

An interesting new use of zeolites lies in their addition of thermoplastic polymers in order to reduce odours and emission of volatile organic compounds (VOC's), as well as in the use of zeolites as carriers of silver particles in polymers or paints. The antimicrobial effect/role of silver ions and their release 'on demand' is used in the production of fabrics/textiles of clothing with odour control. Besides this, the fireproof and UV protection of zeolites are also relevant characteristics that are included in the zeolite's purpose as a filler [53].

Zeolites are used in polymer composites as fillers, which contribute to its strength [54]. In nanocomposite polymers and zeolites, two controversial factors emerge, which have to do with the influence of the zeolite on the composite properties.

One factor [55] is that the inserted zeolite worsens the mechanical properties of the polymer in midst of poor mid-phase interactions between polymers and zeolites. The second factor states that the zeolite yields improved mechanical properties and better behaviour linked to crystallisation, since the polymer chains can pass through the zeolite pores in the nanocomposite materials.

Self healing in dental composites

The study of self-healing materials is biologically inspired where damage initiates a self-directed healing response of smart and self-healing materials. According to healing principles, self-healing polymers and polymer composites can be classified into two categories: intrinsic ones that are able to heal cracks by the polymers themselves, and extrinsic in which a healing agent has to be pre-embedded [56].

In the case of extrinsic self-healing, the matrix resin itself is not a healable one. The initial self-healing system developed by White *et al*. [57] involved the incorporation of a healing agent in an epoxy matrix: microencapsulated monomer dicyclopentadiene (DCPD) and wax microspheres containing Grubbs' catalyst, bis(tricyclohexylphosphine) benzylidene ruthenium (IV) dichloride. When the capsules were broken by an initiating crack, the repair agent from capsules was released and the ring-opening metathesis polymerization (ROMP) occurred (Fig. 9) [58, 59]. Poly (DCPD) is formed in the crack plane, resulting from the ROMP reaction of DCPD initiated by the Grubbs' catalyst to restore the original structural properties of the polymer matrix. This new polymer fills the damaged zones, bridges crack faces, provides crack arrest and recovery of mechanical integrity [61-65]. Further research and investigation were developed in three directions: microcapsules with self-healing agents (SHA) and variation; hollow tubes filled with SHA [66-71]: three-dimensional micro vascular networks [72, 73]. It would be very useful to use this self-healing system in

bone cement materials, which are mostly thermoplastics. Moreover, in the field of these materials, the research should be expanded to the biocompatibility of self-healing agents and products [74-76].
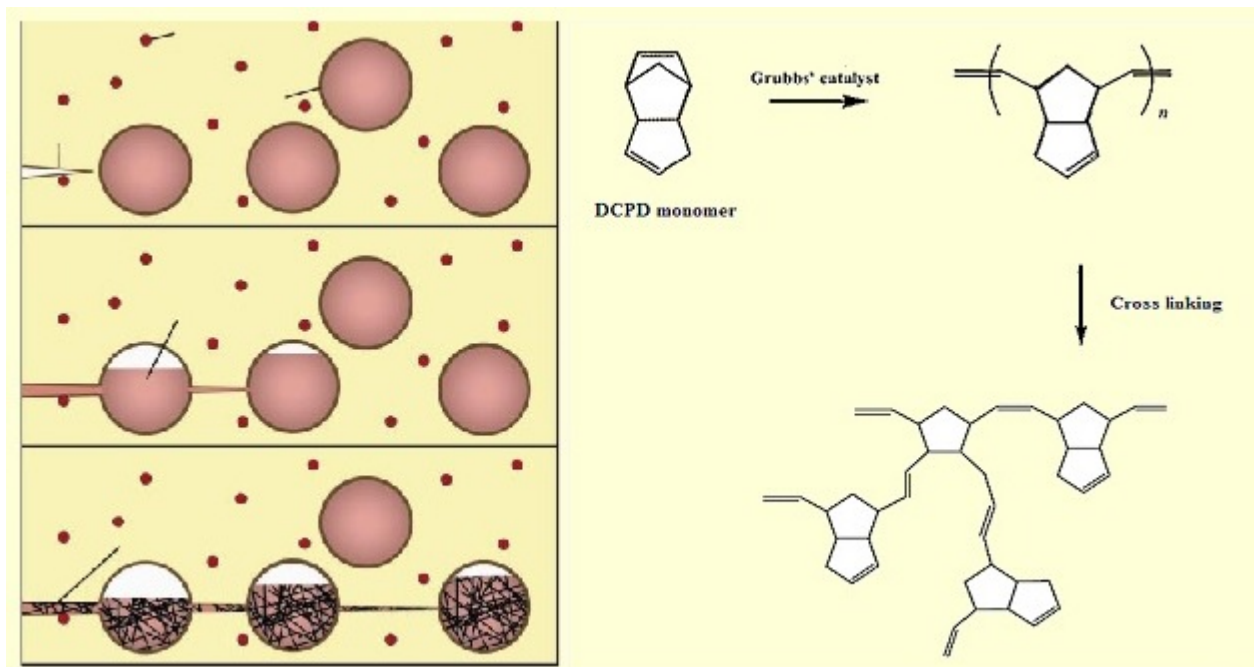
Figure. 9. Ring opening metathesis polymerization of DCPD (After [57])

The aim of this study was to apply a biomimetic approach and to process a material with bleeding ability. The basic principle of this approach lies in filling the brittle-walled containers with a polymerizable medium, which should be fluid at least at the healing temperature. The concept used in this study comprised unidirectional hollow glass tubes with self-healing agents (SHA) in a thermoplastic matrix. During a damage event, some of these hollow tubes may fracture and thus, initiate the recovery of properties by healing. It is also useful to add UV fluorescent dyes into the solution, which could label the damage/healing events that the structure has undergone. In this work, a solution of self-healing agents will be used for filling the tubes [77]. First of all, the choice of an adequate solvent is essential. The selection of solvent is very important because of its viscosity and stability. Namely, it should feed the crack gap in a very short time. The stability and reactivity of the solution should also be preserved.

Coupling agent

A coupling agent is used to achieve good bonding between the inorganic reinforcing fillers and the organic resin matrix. The primary feature of the binding cross-border funds surface modifier reinforcement is to provide a permanent connection between the inorganic filler with an organic polymer matrix. This tool enables hydrolytic degradation by preventing connections filler / polymer and a good distribution of power between polymer and filler.

Bi-functional molecule of silane is attached to the filler with a silanol group by a hydrolysis/condensation reaction that forms covalent bonding. Additionally, radical group is attached to the resin matrix through chemical reaction or chain entanglement [78, 79]. Hydrolytic degradation of the coupling agent may occur in the oral environment and cause inferior properties of the resin composite. Which type of silane will be use is in accordance of polymer matrix nature. For acrylate the most commonly used coupling agent is organosilane 3- methacryloxypropyltrimethoxysilane (MEMO), after that is (3 - aminopropyl triethoxysilane).

The surface of nanoparticles should be modified with the aim to minimize their agglomeration by facilitating their dispersion and achieve the better matrix-particles interface bonding [80]. The alkoxy groups of silane coupling agent react readily with the hydroxyl groups on the surface of alumina whiskers. Owing to their perfect crystal structure, whiskers typically have very high tensile strengths which approach the binding forces of adjacent atoms. So, with the surface modification the area with very good bonding and mechanical properties uniformity could be obtained. Modification of whiskers surface by 3-mercaptopropyltrimethoxy silane (MPTMS) was made in this paper. Among the other silanes, 3-mercaptopropyltrimethoxy silane have showed the good resultes with improvement of thermal and mechanical cyclic life of composites [81].
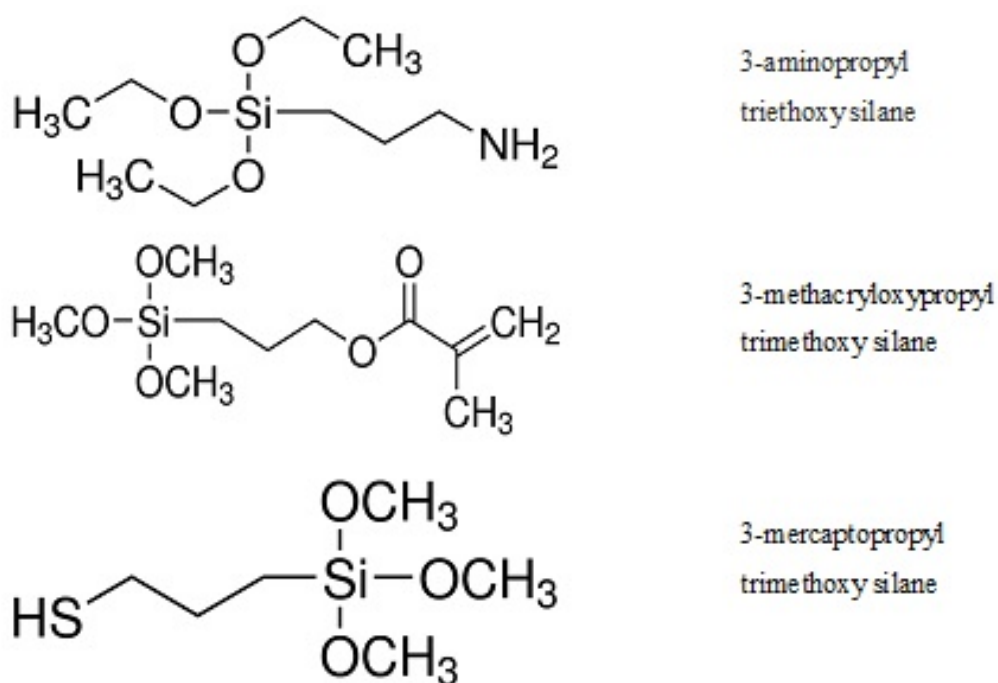
Figure 10. Structural formulas of silanes

The possible interaction between PMMA and modified whiskers is hydrogen bonding between thiol group of silane and carbonyl groups of the polymer matrix [82, 83]. Reaction of MPTMS with alumina whiskers is presented on Figure 11a), while the bonding with PMMA via hydrogen bonding is presented on Figure 11b). To the our best knowledge, this is the first time that 3-mercaptopropyltrimethoxy silane modified alumina whiskers were used in an acrylate. Typically the inorganic acrylic based composite fillers are modified with 3-methacryloxypropyltrimethoxysilane using conventional or supercritical CO_2 methods [84].

Alumina—OH + SH-$CH_2$$CH_2$$CH_2Si(OCH_3)_3$ → Alumina—O—Si—$(CH_2)_3$-SH

a)

Alumina—O—Si—$(CH_2)_3$-SH ······
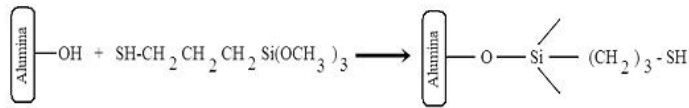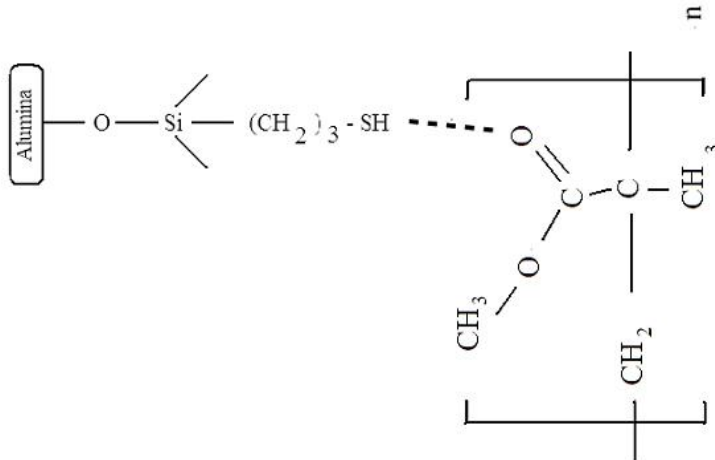
b)

Figure 11. Reactions of a) MPTMS with alumina whiskers; b) silanized whiskers with PMMA

Additional Components of Dental Composite Materials

<u>Polymerization initiators</u> are chemicals that started polymerization of molecular chains by broking some unsaturated bonds.

<u>For light cured</u> a photo-activator is added to accelerate the polymerization reaction. The most commonly used photo-activator is camphorquinone. An acceptable photoinitiator system should fulfill the following requirements:

- High absorptivity in the 300-400 nm range.

- Efficient generation of radicals capable of attacking the olefinic double bond of vinyl monomers.

- Adequate solubility in the binder system (prepolymer + monomer).

- Should not impart yellowing or unpleasant odors to the cured material.

Chemical activation may be achieved by using an organic amine that produces free radicals that expedite the polymerization reaction. Benzoyl peroxide and tertiary amines serve as sources of free radicals. Tertiary amines are most often used as: N, N-dimethyl-p-toluidine and N,N-dihydroxyethyl-p-toluidine.

Pigments are added to match diverse tooth shades, polymerization inhibitors (e.g., 4-methoxy phenol) are added for storage stability, and color stabilizers are added to prevent discoloration with time.

Inhibitors are chemical agents that have the ability to prevent the further polymeriyation . They are chemical agents which work by interfering with the chain initiation and/or chain propagation steps of the polymerisation of the composite material. Most commonly used are monomethyl ether (2-methoxyethanol), hydroquinone or butylated hydroxytoluene.

Stabilisers from UV light or UV absorbers are added for the stability of the composite material's colour. Most often used is 2-hydroxy-methoxybenzophenone.

In recent times, there has been an increased effort to discover new organic-inorganic ingredients that have an improved degree of conversion and the reduction of polymerisation accumulation, therefore increasing resistance of depletion. This type of material is stable with urethane and alkoxysilane, and synthesises using parallel processes: sol-gel process and polymerisation of organic products into a polymer web thus creating an inorganic-organic co-polymer.

Methods of characterization of composite materials

Fourier transform infra-red (FTIR) spectroscopy

The total internal energy of a molecule in a first approximation can be resolved into the sum of rotational, vibrational and electronic energy levels. Infrared spectroscopy is the study of interactions between matter and electromagnetic fields in the IR region. In this spectral region, the EM waves mainly couple with the molecular vibrations. In other words, a molecule can be excited to a higher vibrational state by absorbing IR radiation. The probability of a particular IR frequency being absorbed depends on the actual interaction between this frequency and the molecule. In general, a frequency will be strongly absorbed if its photon energy coincides with the vibrational energy levels of the molecule. IR spectroscopy is therefore a very powerful technique which provides fingerprint information on the chemical composition of the sample. FTIR spectrometer is found in most analytical laboratories. An infrared spectrum represents a fingerprint of a sample with absorption peaks which correspond to the frequencies of vibrations between the bonds of the atoms making up the material. Because each different material is a unique combination of atoms, no two compounds produce the exact same infrared spectrum. Therefore, infrared spectroscopy can result in a positive **identification** (qualitative analysis) of every different kind of material. In addition, the size of the peaks in the spectrum is a direct indication of the **amount** of material present. With modern software algorithms, infrared is an excellent tool for quantitative analysis.

A method for measuring all of the infrared frequencies **simultaneously**, rather than individually, was needed. A solution was developed which employed a very simple optical device called i**nterferometer**. The interferometer produces a unique type of signal which has all of the infrared frequencies "encoded" into it. The signal can be measured very quickly, usually on the order of **one second** or so. Thus, the time element per sample is reduced to a matter of a few seconds rather than several minutes. The resulting signal is

called an **interferogram** which has the unique property that every data point (a function of the moving mirror position) which makes up the signal has information about every infrared frequency which comes from the source. This means that as the interferogram is measured, all frequencies are being measured **simultaneously**. Thus, the use of the interferometer results in extremely fast measurements. Because the analyst requires a **frequency spectrum** (a plot of the intensity at each individual frequency) in order to make identification, the measured interferogram signal can not be interpreted directly. A means of "decoding" the individual frequencies is required. This can be accomplished via a well-known mathematical technique called the **Fourier transformation**. This transformation is performed by the computer which then presents the user with the desired spectral information for analysis. However the FTIR spectrometer operates on a different principle called *Fourier transform*.)
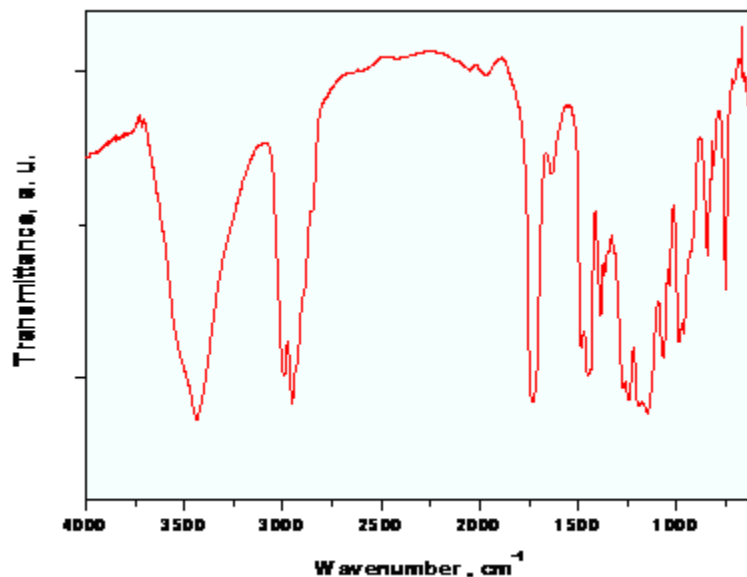

Figure 12 FTIR spectrum of PMMA

Differential Scanning Calorimetry (DSC)

Differential scanning calorimetry (DSC) is an experimental technique to measure the heat energyptake that takes place in a sample during controlled increase (or decrease) in temperature. The DSC can be used to obtain the thermal critical points like melting point, enthalpy specific heat or glass transition temperature of substances. The schematic principle of the DSC is described in Figure 13. This is a thermal analysis with measurement of changes in chemical and physical properties of materials as a function of temperature. The method of differential scanning calorimetry (DSC), is defined as a technique that registers energy or energy flux, necessary to obtain the zero value of the temperature difference between the sample under test and reference substances, as a function of temperature or time, at a predetermined rate of heating or cooling and assuming that the sample and reference substance under the same conditions. In the DSC curves is the area under the peaks directly proportional to the amount of energy exchanged in the process.
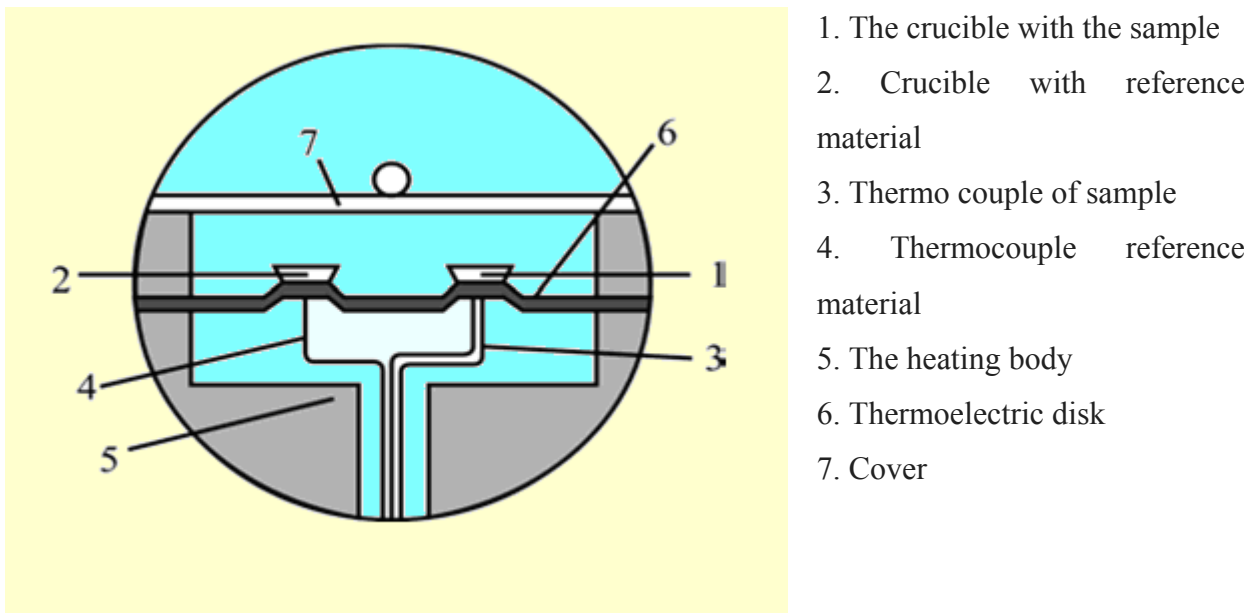

1. The crucible with the sample
2. Crucible with reference material
3. Thermo couple of sample
4. Thermocouple reference material
5. The heating body
6. Thermoelectric disk
7. Cover

Figure 13. Scheme of DSC device

The DSC devices monitor the appropriate changes to the two principles, isothermal or adiabatic. The essence of isothermal approach is ensuring that the temperature of the test sample and the reference temperature materials, maintain equal during the warm-up, or, more rarely, cooling. Therefore, the sample, in order to be at all times at the same temperature as the material in the crucible 2, must be placed in the conditions to be further drained or, if necessary, results in the appropriate amount of heat.

The corresponding change in the heat of the printer is registered as negative or positive deviation from the horizontal position of the base line, so the peaks indicate the endothermic or exothermic effects. This is illustrated in figure no. 14. The signal on the abscissa is proportional to temperature, which is controlled by an additional thermocouple placed in the crucible of the sample. Since it is absorbed, and the energy released is proportional to the heat of reaction, the amplitude peaks immediately indicates the rate of change of - (dH / dt).
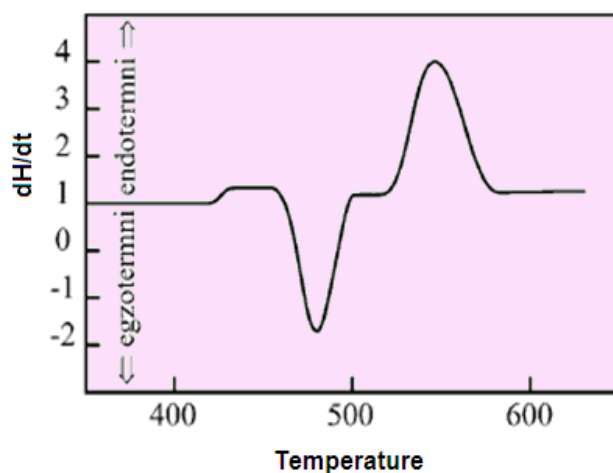

Figure 14. The diagram obtained by DSC analysis

DSC Measurements are used to:

• detection processes that occur in the sample and determine the temperature at which they take place,

• determine the kinetics of individual processes and their activation energy,

43

• determine the change in heat capacity of the sample,

• determine the energy corresponding to the detected processes,

• degree of purity of the substance, etc.

At the simplest level it may be used to determine thermal transition ("melting") temperatures for samples in solution, solid, or mixed phases (e.g. suspensions). But with more sensitive apparatus and more careful experimentation it may be used to determine absolute thermodynamic data for thermally-induced transitions of various kinds. Formerly this was more the realm of the dedicated specialist, but now with the ready availability of sensitive, stable, user-friendly DSC instruments, microcalorimetry has become part of the standard repertoire of methods available to the biophysical chemist for the study of macromolecular conformation and interactions in solution at reasonable concentrations. And, to the extent that thermal transitions might be affected by ligand binding, DSC can provide useful information about protein-ligand binding. The advantages of calorimetric techniques arise because they are based on direct measurements of intrinsic thermal properties of the samples, and are usually noninvasive and require no chemical modifications or extrinsic probes. Furthermore, with careful analysis and interpretation, calorimetric experiments can directly provide fundamental thermodynamic information about the processes involved.

Impact test

The high-speed impact between two bodies is a matter of great importance because many important material parameters have to be determined under this condition. One of the methods used to study the impact behavior of a solid component is the instrumented controlled energy impact. In this test, a striker is dropped from a determined height to have an impact on the sample with the aim of measuring its mechanical response (Figure 15). The striker is instrumented with a load sensor located very close to the impact point, so it is possible to obtain a complete record of the impact event, extracting force–time or force–displacement evolutions. From this record some of the sample mechanical properties, such as the Young's modulus, absorbed energy, the load at break, or the material fracture parameters, can be obtained.

Testing the impact of controlled energy (Impact test) determine the material's ability to withstand loads at different speed. This means that we can control the energy that material undergoes. The test is designed so that the striker with the tip in the form of a hemisphere 12.7 mm diameter penetrates the sample at a controlled rate in the axial direction. The result is obtained in the form of changes of force and energy with time and gives insight into the mechanism of fracture as well as distribution of the energy to the energy of initiation and crack growth.

The phenomenon that occurs during (or on) impact depends on different loads, shown in Figure 16 .   The Force-time diagram can be divided into two phases: the first, when the cracks occurs, and the second, when the breakage (cracks) widens/spreads. As the load increases in the first phase, the energy of elastic deformation gathers in the material as a result, and consequentially leads to cracking on a microscopic scale. At the same time, bending mechanisms on a microscopic level arise (micro-deformation of fibres on the compressed side lead to link breakage between the fibre and matrix, etc.).

When the critical load reaches the end of the first phase, a part of the composite material can be bent because of tension or tangential breakage, depending on the relative value of the interlaminar tension or resistance of shear stress. When this point is reached, the widening breakage can develop catastrophically – just as in the case of brittle materials

(under very heavy load) or in a progressive way – such that they continue to absorb energy (under low pressure/load).

a)

b)

Figure 15. a) High speed puncture impact tester set-up; b) striker and clamping plates inside impact tester

The total impact energy E_t - registered by a device for testing or by an oscilloscope (on the diagram where the time and energy are changing) during load – where E_i is the initial and E_p the widening energy. Brittle materials are defined by high values of initial energy and

low values of widening or absorbed energy (cracking), while strong materials have low values of initial energy of cracking, and high values of widening energy of crack expansion. Knowing the fact that, in summation, brittle and strong materials can have a total impact energy of similar sizes, but it has to be taken into account that the total energy is not enough to explain the behaviour of materials during cracking/breakage.
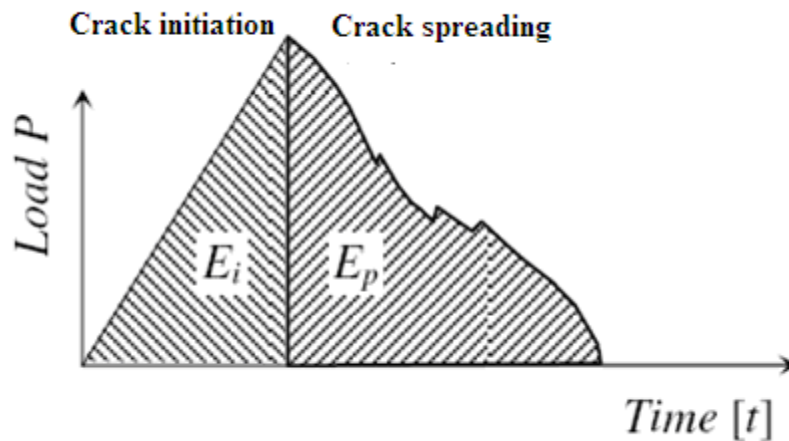

Figure 16. Load-time dependence in impact test. [85]

During the impact of some composite materials, e.g. laminar antiballistic, the complete penetration of the samples could not be occurring, and they were specifically deformed. It was a good opportunity to analyze the deformation and energy absorption during the impact. The impact test results are presented in Figure 17. The force-time-energy curve is marked by the three energy absorption zones [86-88]. The shape of the plots necessitated dividing them into three distinct zones namely, elastic zone (Zone 1), slippage/breakage zone (Zone 2) and failure zone (Zone 3). Zone 1 was found to be almost linear in all the cases and that is the reason behind naming it as elastic zone. The Zone 2 is characterized by fluctuating values of force and it is evident in diagram. These fluctuations are most probably caused by slippage of laminas, exhibiting almost a stick–slip sort of behavior. As during the slippage force cannot increase monotonically, the force curve becomes zigzag (noisy). In untreated fabric, there is too much fluctuation in this zone which does not lead to any additional build-up of force. Zone 3 is characterized by a drop in force which means failure of the structure.
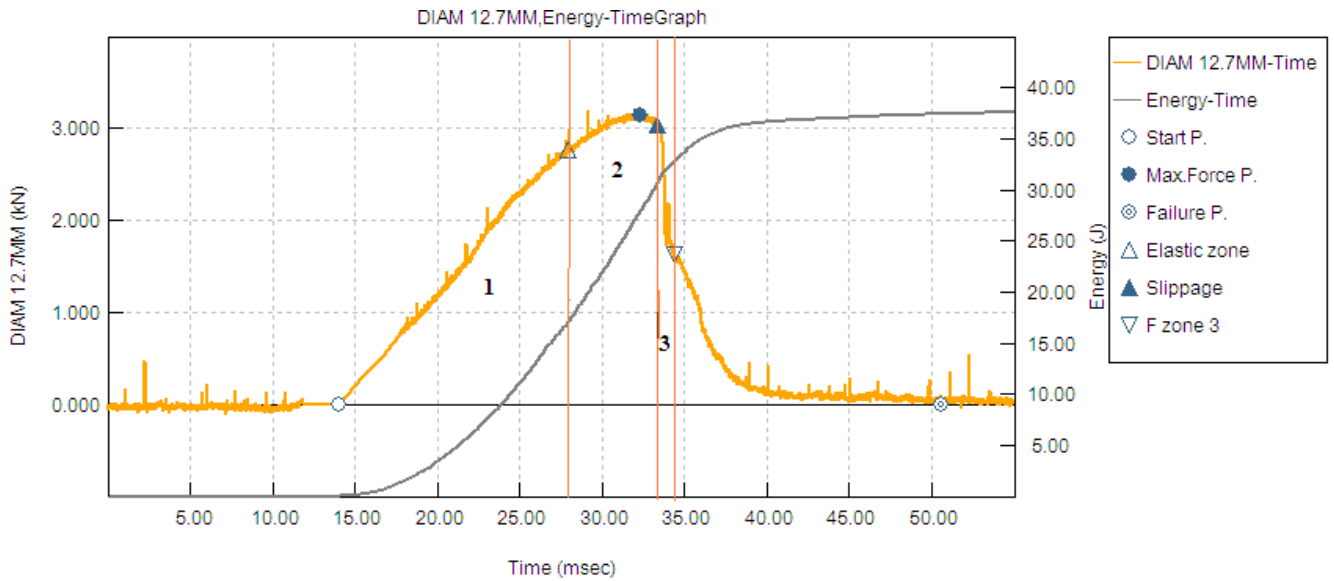
Figure 17. Dependency of Load (Diameter 12.7) and Energy from time

Nanoindentation- determining the elastic modulus and hardness

Since 1992, the analysis method proposed by Oliver and Pharr [89] has been established as the standard procedure for determining the hardness and elastic modulus from the indentation load-displacement curves for bulk materials. In the Oliver-Pharr method, the projected contact area between indenter tip and material is estimated using the equations for the elastic contact of an indenter of arbitrary shape on a uniform and isotropic half space. The indentation modulus and hardness of the material can thus be calculated without the necessity of imaging the indentation after the experiment. The Oliver-Pharr method was initially developed for analyzing indentations in bulk materials, not for films on substrates, and no information about a possible substrate is included in the analysis. The Oliver-Pharr method is, however, frequently used by researchers to interpret indentations performed on thin films in an attempt to obtain approximate film properties regardless of the effect of substrate properties on the measurement. Figure 17 is a typical load

displacement hysteresis curve obtained from an elastic / plastic material and Figure 18 shows the schematic representation of the indent under load and in the unloaded condition. Apart from the measurement of the indenter penetration under the applied force, the unloading contact compliance C (= 1/S) and the contact depth h_c can be calculated. The value of h_c is dependent on the exact shape of the indenter and material response to the indentation; 'sinking-in' and 'piling-up' around the indenter also affect the value.
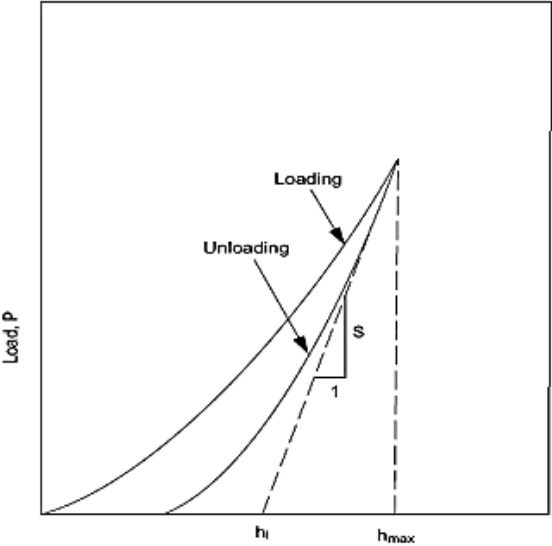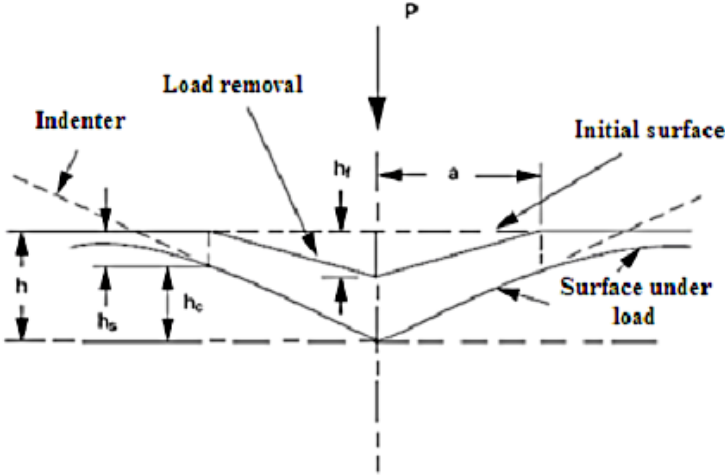
Figure 18. a) Typical force displacement curve showing measured and derived parameters; b Schematic of indentation showing the displacements observed during an indentation experiment [89]

Indentation hardness scale -The indentation hardness H_c is calculated from the test force, P, divided by the projected area of the indenter in contact with the test piece at maximum load:

$$H_c = \frac{P_{max}}{A_c}$$

(1)

where P_{max} is the peak indentation load and Ac is the contact area under maximum load.

The projected contact area A_c is calculated from knowledge of the geometry of the indenter and the stiffness of the contact [90]. In many materials, the area of contact under moderate forces is a good approximation to that which remains when the indenter is fully unloaded and removed from the surface. In such cases, the indentation hardness is very similar to Vickers hardness, the exceptions being that the indentation area is calculated from measured displacement data instead of optical measurement and that the Vickers scale assumes a perfect geometry whereas instrumented indentation uses a measured shape of the indenter which makes allowance for tip rounding and other common deviations. In practice, tip rounding means that the two scales diverge as the indentation contact becomes more elastic until, at the elastic limit, HV becomes infinite and H_{IT} ceases to be a measure of plasticity.

Indentation modulus The indentation modulus E_{IT} is calculated from the slope of the unloading curve through the formula:

$$E_{IT} = \left(1 - v_{IT}^2\right) \Big/ \left\{ \frac{2}{\sqrt{\pi}} \cdot \frac{\sqrt{A(h_c)}}{S} - \frac{\left(1 - v_{indenter}^2\right)}{E_{indenter}} \right\}$$

(2)

where: v_{IT} = the Poisson's ratio of the test piece

$v_{indenter}$ = the Poisson's ratio of the indenter

S = the slope of the tangent of the force/indentation curve during the unloading cycle (Fig. 18a)

h_c = the contact depth value, which is dependent on the shape of the indenter (Figure 18b)

The full procedure for this is described in the draft standard [90]. For homogeneous and isotropic materials, E_{IT} approaches the Young's modulus of the material. For an isotropic material, the value is a 3D average of the crystallographic modulus.

For the analysis of the load-displacement curve the following assumptions were taken:

  a. Deformation upon unloading is purely elastic.

  b. The compliances of the specimen and the indenter tip can be combined as springs in series.

  c. The contact can be modeled using the analytical model developed by Sneddon for the indentation of an elastic half space by a punch that can be described by an axisymmetric solid of revolution.

According to assumption b) the effect of a non-rigid indenter on the load-displacement curve can be accounted for by defining a reduced modulus, Er, by

$$\frac{1}{E_r} = \frac{1-v}{E} + \frac{1-v_i^2}{E_i} \tag{3}$$

where E and v areYoung's modulus and Poisson's ratio for the specimen and E_i and

v_i are the same quantities for the indenter.

During loading the total displacement h is written as

$$h = h_c + h_s \tag{4}$$

where h is the vertical distance along which contact is made (called contact depth), h_s is the vertical displacement of the surface at the perimeter of the contact and h_c is the penetration depth of the indenter under load. When the indenter is withdrawn the final depth of the residual hardness impression under load is h_f. The determination of Young'smodulus is based on Hertz contact equation according to which

$$E_r = \frac{\sqrt{\pi}}{2} \frac{S}{\sqrt{A}} \tag{5}$$

where A is the contact area and S is the stiffness of the unloading curve $(S = dP/dh)$.

According to Oliver and Pharr the unloading data for stiffness measurement are fitted into equation

$$P = B\left(h - h_f\right)^m \tag{6}$$

where P is the load, $(h - h_f)$ is the elastic displacement and B and m are material constants. The quantities B, m and h_f are determined by a least squares fitting procedure of the unloading curve. For the analysis it is assumed that the geometry of the indenter is described by an area function $A = A(h)$ which relates the cross-sectional area of the indenter to the distance from its tip. The contact area at maximum load is given by

$$A = A\left(h_c\right) \tag{7}$$

The contact depth at maximum load, hc, that is, the depth along the indenter axis to which the indenter is in contact with the specimen, is determined by

$$h_c - h_{max} - \varepsilon\left(h_{max} - h_i\right) \tag{8}$$

where h_{max} is the maximum depth and h_i is the intercept depth, that is, the intercept of the tangent to the unloading load-displacement curve at maximum load with the depth axis. The constant ε is a function of the shape of the indenter tip. It takes the value 1 for a flat punch, the value of 0.7268 for a cone indenter and the value of 0.75 for a spherical or parabolic indenter. The quantities h_{max} and h_i are determined from the experimental data.

The area function $A(h_c)$ depends on the shape of the indenter. For a Berkovich indenter it takes the form

$$A\left(h_c\right) = 24.5 h_c^2 \tag{9}$$
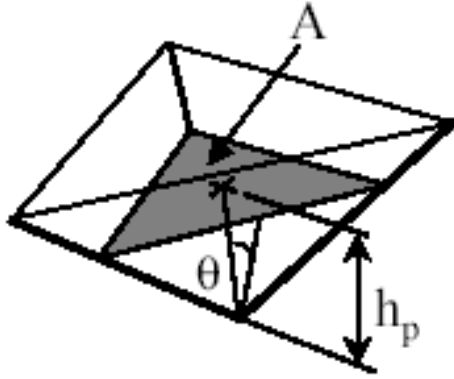
$$A = 3\sqrt{3}\, h_p^2 \tan^2 \theta = 24.5\, h_p^2 \, ;$$

Figure 19. Berkovich indenter and corresponding contact area

The hardness H_c is defined by equation (1). This definition of hardness is different from that used in an imaging indentation test. In the latter case the area is the residual area measured after the indenter is removed, while in the nanoindentation test the area is the contact area under maximum load. This distinction is important for materials with large elastic recovery, for example rubber. A conventional hardness test with zero residual area would give infinite hardness, while a nanoindentation test would give a finite hardness. Equation (9) gives the area function $A_{(hc)}$ for an ideal Berkovich indenter. However, real tips are never ideally sharp and generally, are characterized by a radius of curvature at the tip. In such cases the function $A_{(hc)}$ must be determined. Methods for determining $A_{(hc)}$ include the TEM (transmission electron microscope) replica method in which replicas of indentation are made and their areas are measured in TEM, the SFM (scanning force microscope) method in which the indenter tip is measured with a sharper SFM tip of known shape.

The accuracy of such a measurement depends on the film and substrate properties and on the indentation depth as a fraction of the total film thickness. In general, the error due to the substrate effect increases with increasing indentation depth and with increasing elastic mismatch between film and substrate. To minimize the effect of the substrate on the measurement, the indentation depth is often limited to less than 10% of the film thickness. This empirical rule is not always reliable, especially if the elastic mismatch between film and substrate is large
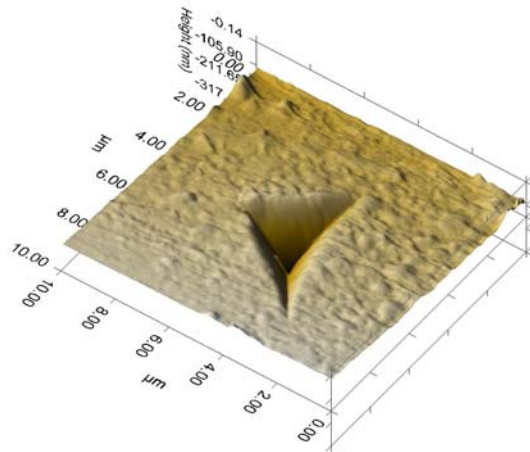
Figure 20. 3D imprint of indent

The 10% rule is also not useful for very thin films when experimental issues make it difficult to obtain accurate results for very shallow indentations. Evidently there exists a need for a method that can be used to analyze thin-film indentation data for indentation depths where the substrate effect cannot be ignored.

Scanning electron microscopy (SEM)

According of formation of imaging and resolution, most microscopes can be classified as one of three basic types: optical, charged particle (electron and ion), or scanning probe. Electron and ion microscopes, use a beam of charged particles instead of light, and use electromagnetic or electrostatic lenses to focus the particles. They can see features as small a tenth of a nanometer (one ten billionth of a meter), such as individual atoms. Scanning probe microscopes use a physical probe (a very small, very sharp needle) which scans over the sample in contact or near-contact with the surface. They map various forces and interactions that occur between the probe and the sample to create an image. These instruments too are capable of atomic scale resolution.

The main components of a typical SEM are electron column, scanning system, detector(s), display, vacuum system and electronics controls (fig. 21). The electron column of the SEM

consists of an electron gun and two or more electromagnetic lenses operating in vacuum. The electron gun generates free electrons and accelerates these electrons to energies in the range 1-40 keV in the SEM. The purpose of the electron lenses is to create a small, focused electron probe on the specimen. Most SEMs can generate an electron beam at the specimen surface with spot size less than 10 nm in diameter while still carrying sufficient current to form acceptable image. Each point on the specimen that is struck by the accelerated electrons emits signal in the form of electromagnetic radiation. Selected portions of this radiation, usually secondary (SE) and/or backscattered electrons (BSE), are collected by a detector and the resulting signal is amplified and displayed on a TV screen or computer monitor. The electron beam interacts with the specimen to a depth approximately 1 μm. Complex interactions of the beam electrons with the atoms of the specimen produce wide variety of radiation. The need of understanding of the process of image formation for eliable interpretation of images arises in special situations and mostly in the case of high magnification imaging. In such case knowledge of electron optics, beam-specimen interactions, detection, and visualization processes is necessary for successful utilization of the power of the SEM.

FESEM is the abbreviation of Field Emission Scanning Electron Microscope. A FESEM is microscope that works with electrons (particles with a negative charge) instead of light. These electrons are liberated by a field emission source. The object is scanned by electrons according to a zig-zag pattern. A FESEM is used to visualize very small topographic details on the surface or entire or fractioned objects. Electrons are liberated from a field emission source and accelerated in a high electrical field gradient. Within the high vacuum column these so-called primary electrons are focussed and deflected by electronic lenses to produce a narrow scan beam that bombards the object. As a result secondary electrons are emitted from each spot on the object.
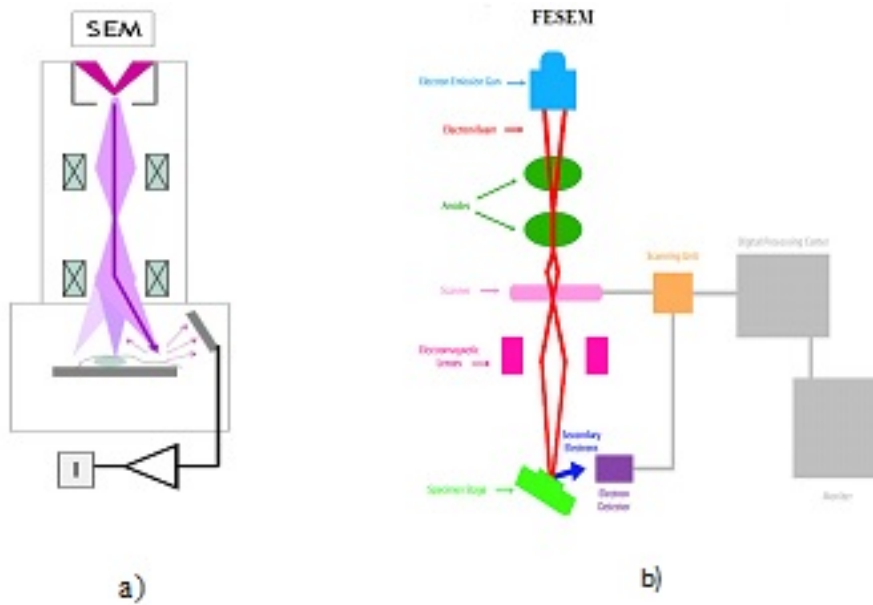
Figure 21. Scheme of forming imaging of a) SEM; b) FESEM

The angle and velocity of these secondary electrons relates to the surface structure of the object. A detector catches the secondary electrons and produces an electronic signal. This signal is amplified and transformed to a video scan-image that can be seen on a monitor or to a digital image that can be saved and processed further. In standard electron microscopes electrons are mostly generated by heating a tungsten filament by means of a current to a temperature of about 2800°C. Sometimes electrons are produced by a crystal of lanthanum hexa boride (LaB_6) that is mounted on a tungsten filament. This modification results in a higher electron density in the beam and a better resolution than with the conventional device. In a field emission (FE) scanning electron microscope no heating but a so-called "cold" source is employed. An extremely thin and sharp tungsten needle (tip diameter 10–7 −10-8 m) functions as a cathode in front of a primary and secondary anode. The voltage between cathode and anode is in the order of magnitude of 0.5 to 30 KV. Because the electron beam produced by the FE source is about 1000 times smaller than in a standard microscope, the image quality is markedly better

The perspective of composite materials in dentistry

The selection of a restorative material has significantly changed in recent years. These restorations use specially fabricated materials to help restore the tooth structure. Restoration or dental filling materials are commonly used for applications such as i) to fill and repair dental caries and cavities, ii) cementation of dental prosthesis, and iii) surgical restoration due to external trauma. Restorations are also increasingly used for cosmetic purposes such as reconstruction of anterior teeth, correction of stains and erosion, and alignment of teeth.

The use of composite resins has grown significantly internationally as a material of choice for replacing amalgam as a restorative material for posterior restorations. This demand is partially consumer driven by preference for esthetic materials and the concerns regarding the mercury content of amalgam. It is also driven by dentists recognizing the promise of resin-based bonded materials in preserving and even supporting tooth structure. Numerous studies have suggested that bonding the restoration to the remaining tooth structure decreases fracture of multi-surface permanent molar restorations.

This state-of-the discussion of composite materials in dentistry is examined in terms of biological materials for fabrication of tissue engineering, nanoengineering, self-assembling systems. For these roles the composites in dentistry should satisfy not only mechanical demands, but also functionality. This means, that the resin could be improved by functional nanomodification in direction of tissue development and protection and also in some perspective of self healing.

In this research some perspectives and possibilities are explored with fictionalization of auto polymerized acrylic resin for use in dentistry.

EXPERIMENTAL PART

SYNTHESIS AND CHARACTERIZATION OF FUNCTIONAL COMPOSITE MATERIALS FOR APPLICATIONS IN DENTISTRY

Materials and methods

Materials

A chemically (self)-cured auto polymerizing resin, Simgal-R$^®$ (Galenika, Serbia) was used as polymer matrix. It is a two component system, including a powder and a liquid. The powder consists of a PMMA copolymer and the initiator benzoyl peroxide (BPO) in a concentration of 1.1 % w/w. The number average molecular weight of the Simgal powder obtained from gel permeation chromatography measurements was 116000 g mol^{-1}, with a polydispersity of 4.54. Size exclusion chromatography measurements were performed using a Waters HPLC system with an RI detector and a set of four styragel columns. Chloroform was used as the eluent with a sample concentration of 10 mg ml^{-1} and mobile phase flow rate 1 ml min^{-1}. Calibration was performed using polystyrene standards. The liquid consists of methyl methacrylate (calc) 94.15 % w/w; acid as methacrylic acid 19.8 ppm w/w; *N,N*-dimethyl-*p*-toluidine as accelerator 0.85 % w/w; ethylene glycol dimethacrylate as cross linking agent 5.00 % w/w; water 27 ppm w/w.

The alumina whiskers were commercially available from Sigma–Aldrich, and they were characterized by diameters of 2–4 nm and lengths of 200–400 nm (specified by the producer). 3- mercaptopropyltrimethoxy silane (MPTMS, 95 %; Sigma–Aldrich.) was used as a coupling agent.

The particles of Zeolite 4A were commercially available from Silk, Slovenia.
The chemicals that were used in preparing the self-healing system: dicyclopentadiene, (DCPD), 95 %, stabilized, ACROS Organics; dimethylformamide, (DMF), 99.8 %, Sigma–Aldrich; Rhodamine B (RhB), Sigma–Aldrich, M = 479.01 g mol^{-1}; Grubbs' catalyst 1st

generation, Sigma–Aldrich, bis(tricyclohexylphosphine) benzylidene ruthenium(IV) dichloride; dichloromethane (DCM), Sigma–Aldrich.
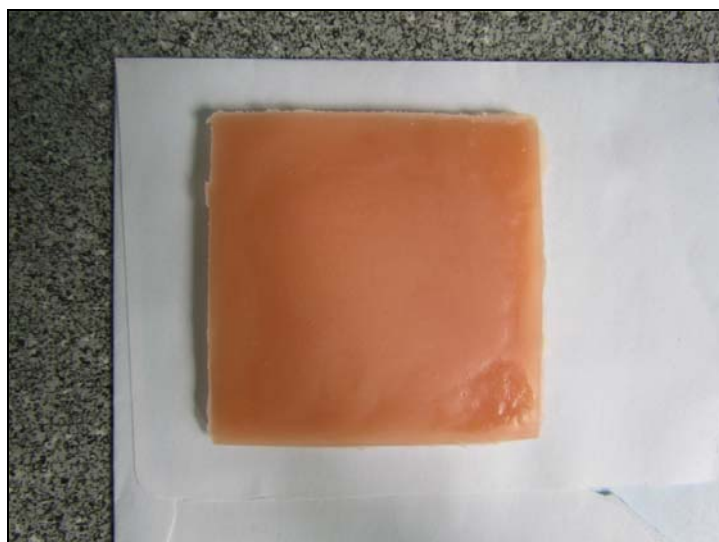
Preparation of samples

The samples were prepared with a powder to liquid ratio of 2:1 in weight and subsequently cast in silicon molds on mixing the polymer powder and liquid monomer, the initiation/induction process commenced (primary radical formation). This is followed by a repeated propagation sequence, the addition of monomer to an active center (free radical) to generate a new active center. Monomers add sequentially to the end of a growing chain by repeated head to tail addition. It ends with termination whereby poly (methyl methacrylate) chains are formed. The free radical polymerization reaction produces high molecular weight PMMA polymers and is very fast and exothermic.

The samples with particle filler were prepared in the same manner with additional mixing when the particles were added in mixture for polymerization. The series with different composition were processed: pure acrylic resin (AR), with 3 % w/w [37] unmodified whiskers (ARW) and with 3 % w/w modified whiskers (ARWMPTMS). The nanocomposites were prepared to follow: the proper amount of whiskers was added after mixing powder and liquid. Molds were left for 48 h at room temperature. The samples with Zeolite were prepared in the same manner. Three Series with different content of Zeolite were processed: with 1 % wt, 3 %wt., 5 %wt.
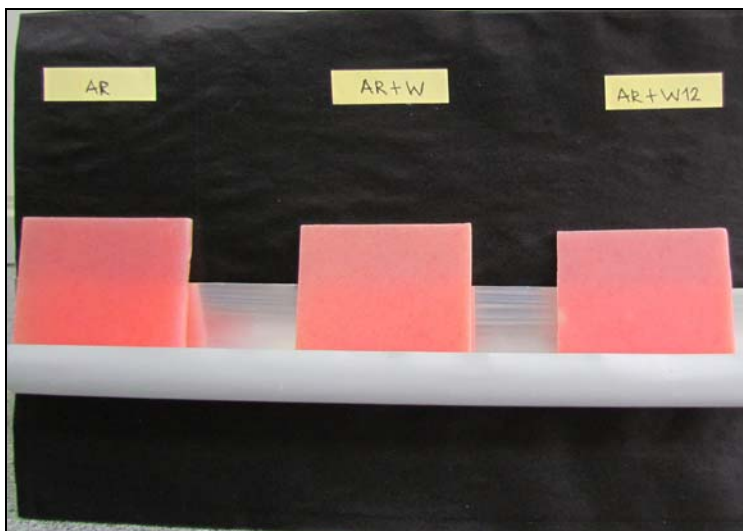
Figure 22. Samples with alumina whiskers

Figure 23. Sample with Zeolite 1 % wt.

Modification of alumina whiskers surface

The thiol group grafted samples were prepared as follows: 0.6 ml of MPTMS was mixed with 1.5 g of alumina whiskers in 50 ml of dried toluene. This mixture was stirred under reflux condition for 36 h. Then the solid in the mixture was collected by filtration, rinsed with anhydrous ethanol to remove the non reacted MPTMS and dried at 80 ºC for 24 h according literature [91]. The unmodified whiskers were denoted as W, while modified whiskers as WMPTMS.

Preparation of the self healing (SH) specimens

Ten hollow glass tubes, with inner diameter of 0.8 mm and 50 mm length, were filled with two kinds of solutions. Five of them were filled with a 10 wt. % solution of DCPD in DMF, to which 0.5 wt. % laser dye RhB was added.

The other five tubes contained 1 wt. % solution of Grubbs' catalyst in DCM. Their ends were closed with plasticine. DMF and DCM were chosen because they exhibited the highest healing efficiencies after screening for solvent healing ability [92].

Into a dry and clean glass test container, Simgal liquid was poured and the powder was added until saturation was achieved, lasting no longer than 15–20 seconds (according to the manufactures script). Mixing was performed in 40–45 seconds. The first half of the mass material was poured into a silicone mold. Tweezers were used to place the prepared glass tubes in the middle of the sample, alternatively, monomer–catalyst–monomer tube. Their position was parallel to one another, at a distance of approximately 2 mm (Fig. 23). Then they were covered with the remaining half of the material. The specimens were stored for 20 min until the polymerization was completed. The specimen dimensions were 60 x 60 × 3.5 mm.

DCPD in DMF
+
Rh B

a)

Grubbs in DCM

poly (DCPD)

b)
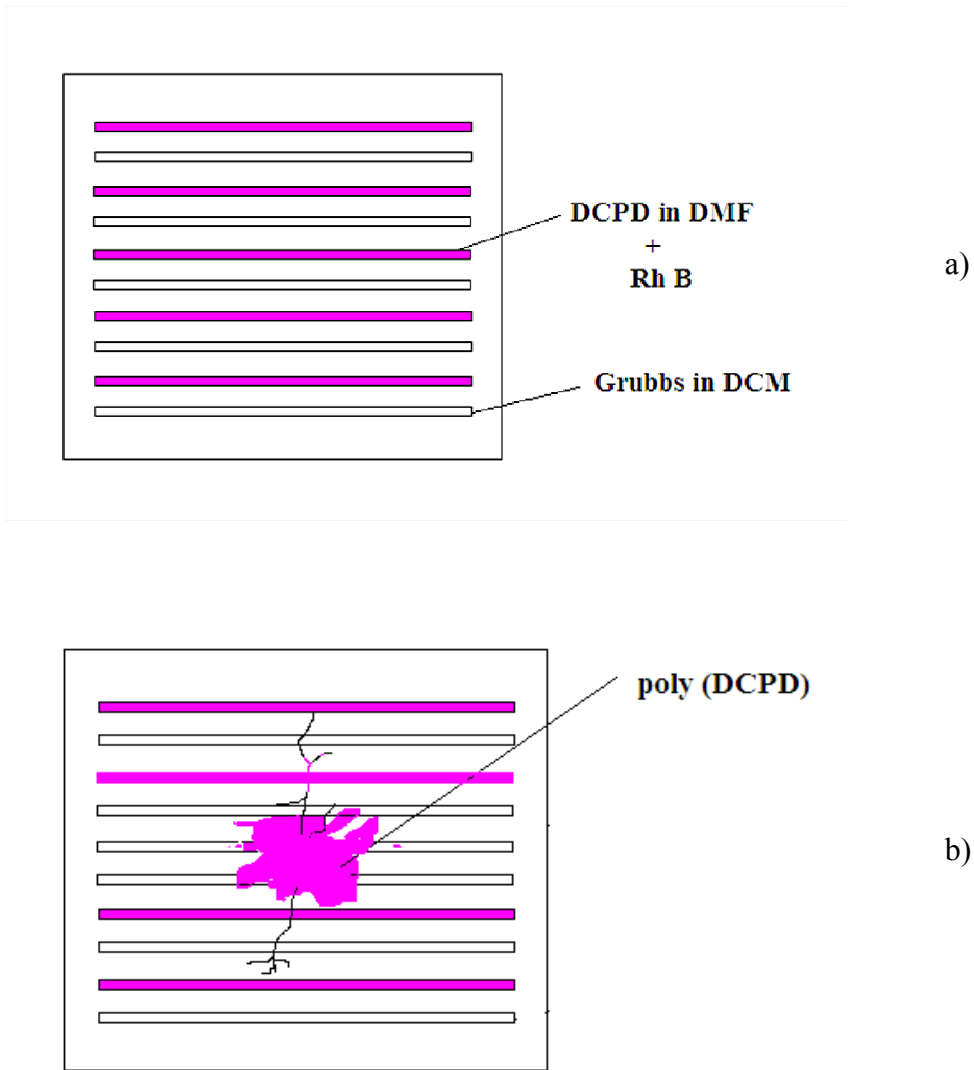
Figure 24. a) Scheme of ordering of the tubes in a composing sample; b) Principles of self-healing

The preparation of specimens was performed at room temperature 21 $^\circ$ ± 2 ℃. Higher temperature shortens, and lower temperature prolongs the working time, which is 3–4 minutes.

Figure 25. A cross section of a sample with a) empty glass tubes and b) after SH

The three series of specimens were processed: Series 1. - original, acrylic resin without tubes, Series 2. - control, acrylic resin with empty tubes, Series 3. - self-healing, with filled tubes. The cross section of sample with empty tubes is presented in Fig. 24. The samples were prepared in order to establish the mechanical behavior before and after pseudo-impact damage. An objective of this study was to establish the efficiency of repair after a period of time had elapsed.

Methods of characterization

Fourier transform infrared (FTIR) spectra of the samples in KBr discs were obtained by transmission spectroscopy (Hartmann & Braun, MB-series). The FTIR spectra were recorded between 4000 and 400 cm^{-1} wavenumber region at a resolution of 4 cm^{-1}. The starting reactants were analyzed as received (RhB and DCPD) or in the starting solutions (DCPD in DMF and Grubbs' in DCM). The sampling for poly(DCPD) was obtained by scratching the self-healed violet bleed.

Differential scanning calorimetry (DSC) measurements were conducted using a DSC Q10 TA Instruments, calibrated to indium standards. Samples of 5 mg were investigated. The measurements were performed under a dynamic nitrogen flow of 50 ml min^{-1} in the temperature range from 30 °C to 200 °C. The samples were heated up to 200 °C at a rate of 10 °C min^{-1}, kept at 200 °C for 5 min to erase thermal history and then cooled to 30 °C at the same rate. A second heating was performed on the each sample. The glass transition temperature was determined as the midpoint of the initial slope change. The T_g values were confirmed by the use of the derivative curve.

Controlled impact energy tests were performed on High Speed Puncture Impact testing machine HYDROSHOT HITS-P10 (Figure 26). The clamping plates with a hole diameter of 40 mm and clamping pressure of 0.55 MPa were used. The striker with a hemispherical head, diameter 12.7 mm, was loaded with programmable velocity, height and attained a value of depth. In this manner it is possible to control the impact energy. The data for the force, deflection, velocity and energy with time were recorded. The impact speed was set at 0.1 m/s and load was 10 kN. The samples of all series were investigated by impact test. Samples of Series 3 were first impacted, left for 96 h and then re-impacted again at the same location. The data were analyzed in terms of peak load, energy to peak load and total energy.
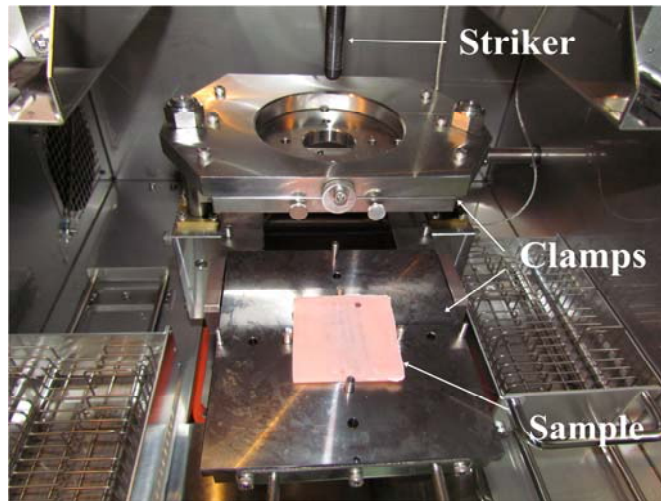
**Figure 26. The sample in machine for impact test**

Nanoindentation tests on the virgin and healed surfaces of the same sample were performed using a Hysitron TI 950 TriboIndenter equipped with *in situ* SPM imaging (Hysitron, MN). The Berkovich indenter has an average radius of curvature of about 100 nm. The positions of nanoindentation were one without crack and the other on the healed crack surface. The hardness and reduced elastic modulus were calculated from the curves using the Oliver and Pharr method [89]. The indentation maximum load was set to be 0.5 mN for all tested samples. The loading and unloading times were set to 20 s each and the hold time at the peak force was set to 10 s. In order to obtain reliable statistical data, at least 9 indentations were made on each sample.

Results and Discussion

Composites with alumina whiskers

FTIR analysis of alumina composite

The silanization of whiskers was followed by the FTIR spectrum of unmodified and modified whiskers (Figure 27). The FTIR spectrum of MPTM silane is also presented on Figure 26.
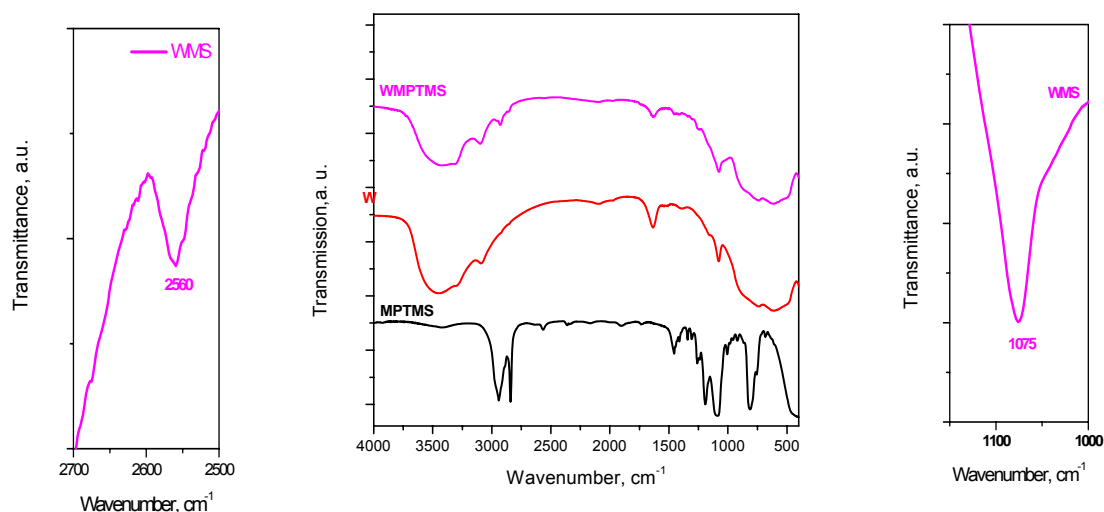
Figure 27. FTIR spectrum of MPTMS silane, whiskers (W) and silanized whiskers (WMPTMS). The enlarged parts are from WMPTMS spectrum [83]

The band at 2560 cm^{-1} observed in the spectrum of WMPTMS is assigned for the S–H stretch band [93, 94], which was not observed in the absorption spectrum of unmodified alumina whiskers, indicating that MPTMS was grafted on the whiskers surface [95, 96]. The absorption bands for the propyl group are appearing at 2936 and 2852 cm^{-1} due to the C–H stretching vibrations, further justifying the MPTMS anchored onto whiskers.

Additionally, the band in the 1075 cm^{-1} is assigned to the vibration of Si–O–Al bond [97, 98]. These facts indicate that chemical immobilization of MPTMS on nano whiskers was successfully occurred [95-98].

Morphology of alumina composite (FESEM analysis)

FESEM photos of the composite fracture surfaces of bulk samples with unmodified (a) and modified (b) whiskers are presented in Figure 28. The composite with modified whiskers had smoother surfaces, with individual whiskers well dispersed in the resin matrix and well defined active bonding (needle like) areas [99,100]. Otherwise, the sample of composite with unmodified whiskers have shown a great agglomeration of particles up to 1 µm.The FESEM photos revealed that silanization of particles leads to better deagglomeration of particles.
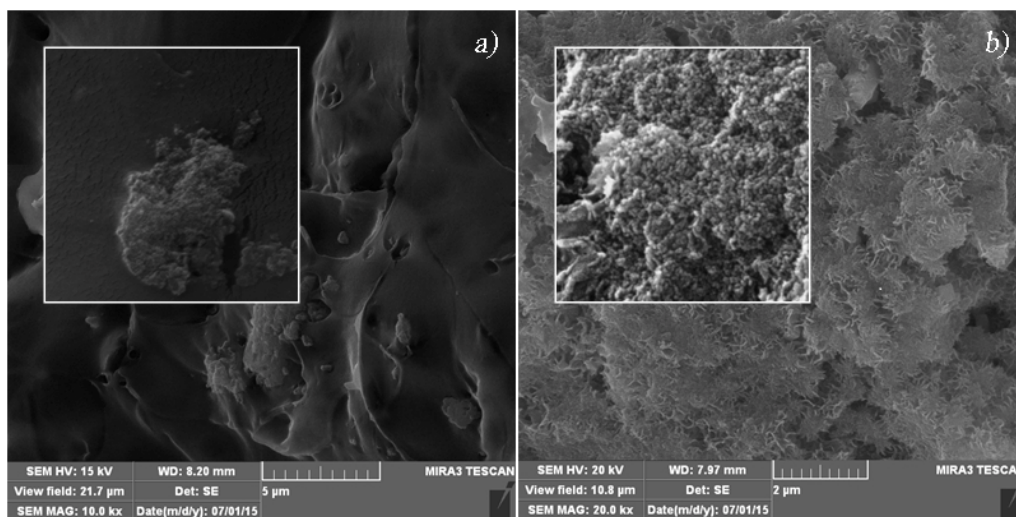

Figure 28. FESEM of samples fractures for: a) ARW; b) ARWMPTMS [83]

DSC analysis of alumina composite

Results of DSC analysis of Simgal and nanocomoposites are presented in Fig. 29. The glass transition temperature T_g of Simgal as an auto polymerized denture base polymer was considerably lowered - 84.02 °C because of the residual MMA content [101, 102]. Even in the absence of specific interactions with the polymers, whiskers behave as highly functional physical cross links and hence reducing the overall mobility of the polymer chains [103, 104]. So, the T_g of ARW is slightly higher than pure resin – 86.14 °C. The nanocomposite thermal behavior's dependence appears to be a function of the added polymer/nanoparticle interfacial area and the T_g of ARWMPTMS is more increased (86.49 °C). Alumina/PMMA composites have been shown reduced glass transition temperature (T_g) at extremely low alumina contents [104]. But, for higher content of alumina the glass transition temperature (T_g) of the composite has been increased as compared to that of virgin polymer [105, 106].
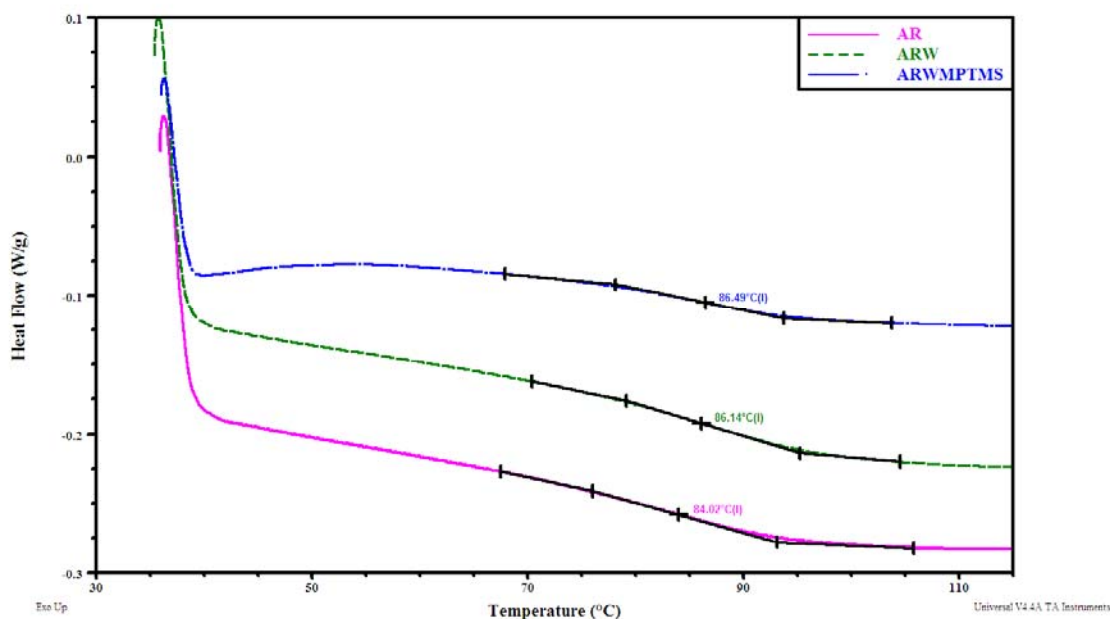

Figure 29. DSC analysis of AR, ARW and ARWMPTMS [83]

**Nanoindentation test of alumina composite**

Figure 30a shows typical force–depth curves obtained in the nanoindentation tests for neat PMMA film and composites with alumina whiskers and MPTMS treated whiskers. The curves appear to be with continuity and without pop in or pop out in both - loading and unloading phase. Figures 30 (b-d) display the plastic imprint of the indent for the AR, ARW and ARWMPTMS samples with the scan trace in the vicinity of the indent. In-situ imaging mode used for scanning the surface trace reveals the absence of cracks and fractures around the indent. Line traces shows small piling-up along the edges, but in addition to the film surface roughness (adequate, but not ideal); these scans raise the confidence that nanoindentation tests captured actual material properties. The results of reduced elastic modulus (E_r) and hardness (H) are presented in Table 1. The reduced modulus for composite with untreated particles increases to 54%, while the hardness is increased to 60% in comparison the neat PMMA films. For composites with MPTM silane treated particles the modulus increases for about 65% and hardness increase is about 90%. From these results it can be concluded that dispersion of the nanowhiskers in the polymer matrix is one of the most important factors controlling the E_r and H improvement in polymer nanocomposites. Elongated structures make the entire surface of whiskers available for the polymer and maximize polymer–whiskers interactions, increasing the reinforcement. Additional factor playing a role in enhancing the nanocomposite mechanical properties include the organic modification of the whiskers and the addition of compatibilizers to the polymer matrix. The increased resistance to surface deformation of the PMMA nanocomposites may be due to a decrease in the free volume of the matrix associated with the formation of apparent physical cross linking and entanglements. For composites with silane treated particles, the results are comparable to those with other nanoparticle composites which achieved favorable dispersion and particle matrix bonding [99, 107].
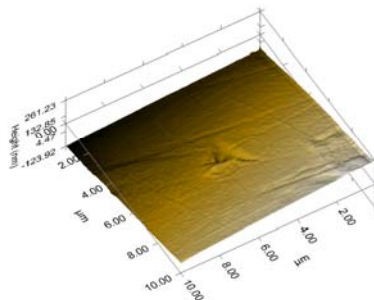
Table 1 *Results of nanoindentation*

	Er, GPa	St.Dev,GPa	H, GPa	St.Dev,GPa
AR 0	5.56	± 0.45	0.26	± 0.035
ARW	8.55	± 0.82	0.43	± 0.061
ARWMPTMS	9.35	± 1.03	0.50	± 0.073
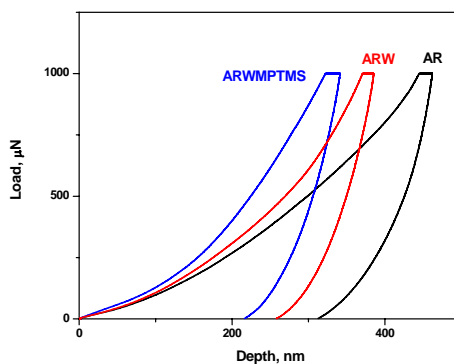
a)
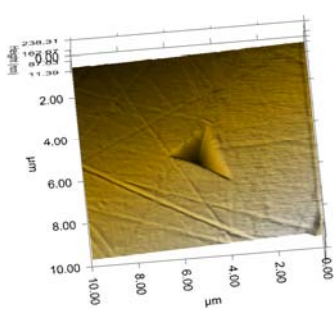
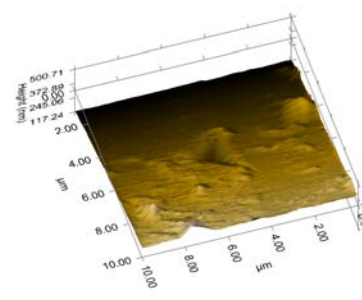b)   c)   d)

Figure 30. a) Load–displacement curves of neat AR and nanocomposite films; b) Indent plastic imprint with scan trace of the pure AR sample; c) Indent plastic imprint with scan trace of ARW sample d) Indent plastic imprint with scan trace of ARWMPTMS sample [83]

Impact test of alumina composite

The results of impact tests are presented in Figure 31. The load-time curves in Fig. 31 a are presented for samples of all three series: AR, ARW and ARWMPTMS. In Table 2 the data for maximum force (F_{max}), totally absorbed energy (E_{tot}) and slope of the elastic region in load-displacement curve are presented.

It can be seen from the Table 2 that the absorbed energy for sample with unmodified whiskers is lower than pure AR. For sample with modified whiskers the absorbed energy is the highest. The reason for this behavior is that there is no bonding between whiskers surface and polymer matrix. The end of whiskers acts as a generator of nano-micro cracks in a composite. With modification of whiskers by MPTMS there is chemical bonding with polymer matrix and the better impact behavior is achieved. The slope of the force–displacement curve in the elastic zone or the flexural specimen compliance was obtained by Data processing Software. This slope is proportional to the modulus of elasticity [108, 109] and it was increased with the addition of modified whiskers (Table 2).

Increase in the mechanical properties of the samples with pre-silanized alumina whiskers can be probably due to physico-chemical interactions between silane group on the microcapsules' shell and hydroxyl groups of the acrylic-based polymeric matrix.

Table 2 Results of impact tests

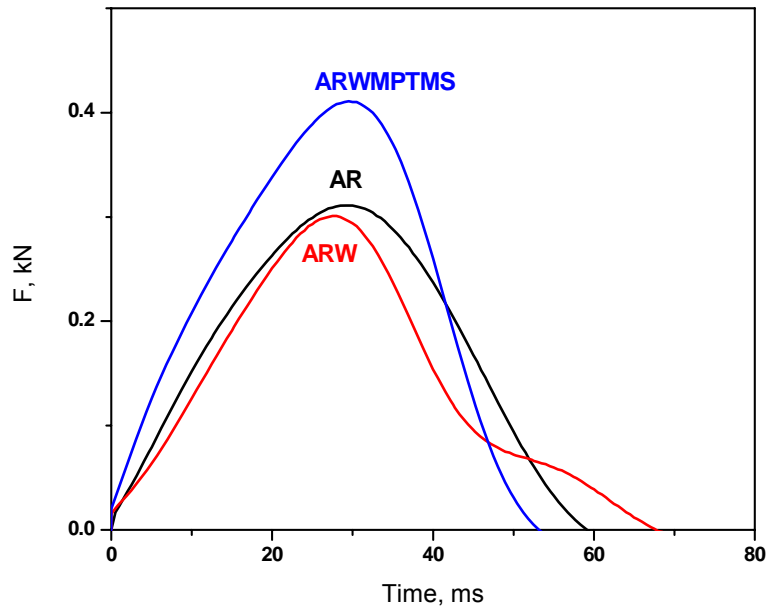| Series	F_{max}, kN	E_{tot}, J	Slope, kN/mm
AR	0.31	1.10	0.13
ARW	0.30	0.93	0.13
ARWMPTMS	0.41	1.30	0.20

Figure 31. The load-time curves of the AR, ARW and ARWMPTMS; [83]

Composites with Zeolite

DSC Analysis of Zeolite composite

The results of DSC analysis for pure Simgal and Zeolite composite are presented in Figure 32. DSC analysis revealed that pure Simgal shows a T_g at 75, 65 ° C, which is significantly lower than the Tg of pure PMMA. This lowering of Tg is assumed that the presence of moisture. A sample of the samples showed T_g at 71.64 ° C. On the curve for the sample with Zeolite appears peak, which is assumed to be due to the presence of residual peroxide polymerization as well as monomers.
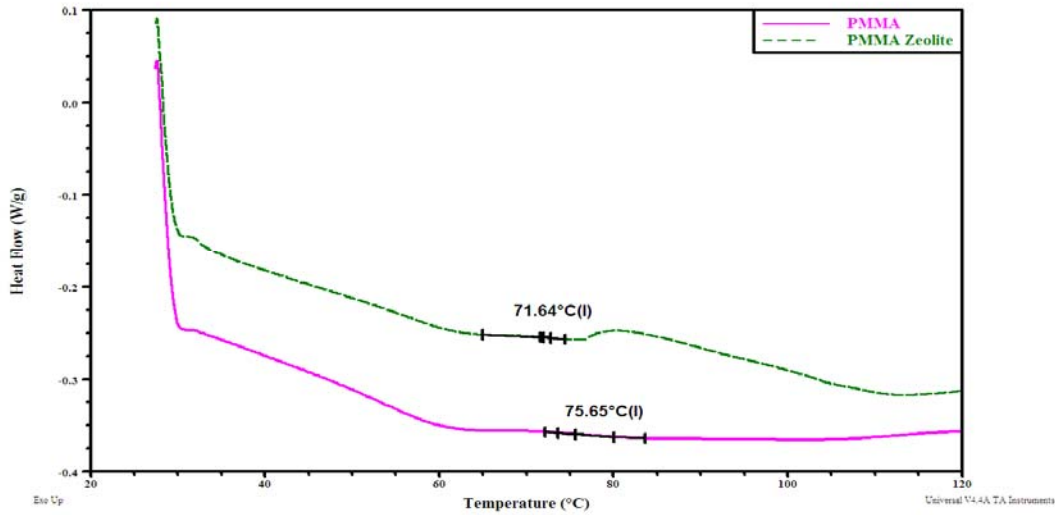
Figure 32. The Results of DSC Analysis

Impact test of Zeolite composite

The impact test results are shown in Figure 33 and Tables 3-6. It is evident that the addition of Zeolite 4A in Simgal increasing absorbed energy and fracture toughness. Also, with the increasing of zeolite content in the composite increases energy absorbed, maximum force, while the penetration depth at maximum force decreases. It can be seen that the slope of load-depth curve, which is proportional to modulus of elasticity, raised as the content of Zeolite raised (Tables 3-6).

These results indicate that the addition of Zeolite improved mechanical properties of acrylic resin, and its structure allows functionalization of dental composites. In fact, if you make it through Zeolite insert certain ions, for example silver, their release to get the composite with antimicrobial properties.
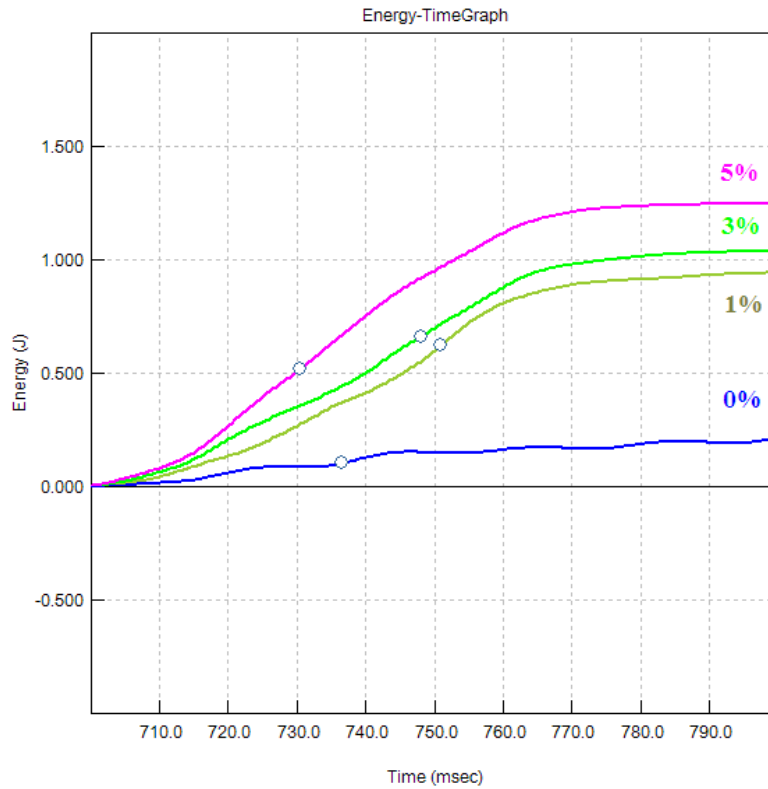
Figure 33. Dependence Of The Energy- Time During Impact test

Table 3. Test results for Simgal

	Energy	Depth	Force	Slope
	J	mm	kN	kN/mm
Start	0	0	0	
Max.Load	0.43	5.5	0.19	0.03
Puncture	1.16	9.7	0.05	

Table 4. *Test results for Zeolite 4A 1 %*

	Energy	Depth	Force	Slope
	J	mm	kN	kN/mm
Start	0	0	0	
Max.Load	0.62	5.4	0.21	0.06
Puncture	0.94	9.8	0.02	

Table 5. *Results of tests for Zeolite 4A 3 %*

	Energy	Depth	Force	Slope
	J	mm	kN	kN/mm
Start	0	0	0	
Max.Load	0.66	4.9	0.23	0.09
Puncture	1.04	9.9	0.01	

Table 6. Results of tests for Zeolite 4A 5 %

	Energy	Depth	Force	Slope
	J	mm	kN	kN/mm
Start	0	0	0	
Max.Load	0.72	3.2	0.25	0.13
Puncture	1.26	9.3	0.02	

Composites with self healing (SH) characteristics

FTIR analysis can be performed to follow the success of the self-healing process. For this investigation, the FTIR analyses were performed on the dental restorative acrylic material, Simgal, and the starting reactants for charging the tubes: DCPD in DMF and Grubbs' in DCM, and RhB. Finally, after the self-healing process, the colored violet bleeds-healed polymer was extracted from surface for FTIR analysis. The results of FTIR analyses are presented in Fig. 34a. Enlarged part of the spectra for DCPD, Simgal and the healed bleed are presented in Fig. 34b. The spectrum bands of the DCPD monomer at 1572 and 1614 cm^{-1} are assigned to the v(C=C) stretching vibrations of the norbornene and cyclopentene double bonds. In the references that describe an investigation of the polymerization of DCPD by FT-Raman spectroscopy, there are information and presumption of presence of the stretching vibrations near 1614 cm^{-1} in the monomer of PCDP regarding the opening of

the norbornene ring, which influences ring tension and stabilization in cyclopentene ring [110, 111]. The 1572 cm^{-1} peak was absent from the FTIR spectrum of the ring-opened poly(DCPD) in the bleed. The peak at 1614cm^{-1} was shifted to 1620 cm^{-1} in the spectrum of poly(DCPD). Moreover, the intensity increased of the band at 1653 cm^{-1}, assigned to the v(C=C) stretching vibrations of the aliphatic double bonds in the polymer chain [110, 111].

The intense, sharp peaks at 754 cm^{-1} and 726 cm^{-1} represent the *cis*-RCH=CHR bending modes. The lowering of the peak at 754 cm^{-1} and almost loss of the peak 726 cm^{-1} as well as the growth of a new peak at 966 cm^{-1} are evidence that the polymerization of DCPD had occurred [112, 113]. The new peak is the representative of the C–H bending mode of a trans-double bond.

The spectrum of Simgal exhibited vibrational bands typical for PMMA, *i.e.*, vibrational bands at 987 and 1453 cm^{-1} that belong to O–CH$_3$ bending and stretching deformation of PMMA, respectively. A band at 1731 cm^{-1} was assigned to stretching of the C=O group and that at 1250 cm^{-1} was assigned to stretching of the C–O group. A band at 1065 cm^{-1} could be ascribed to the C–O stretching vibration and a band at 1197 cm^{-1} belongs to the skeletal chain vibration. The other bands appearing in 3000 – 2800 cm^{-1}, 1490 – 1275 cm^{-1} and 900 – 750 cm^{-1} spectral regions correspond to different CH$_3$ and CH$_2$ vibrational modes [114]. During the polymerization reaction of the acrylic resin, uncured monomer, called residual monomer, is remains [115-120]. A band at 1637 cm^{-1}, assigned to methyl methacrylate monomer (MMA), appeared in spectrum of Simgal. It was assumed that the residual MMA monomer underwent polymerization using the Grubbs' as tandem catalysis for ROMP and atom transfer radical polymerization (ATRP) [121, 122]. In the present system of matrix and self-healing agents in solution, the solution content of the tubes served as reservoir for both polymerizations [123-128].

Moreover, the ROMP polymer can be engaged in the radical polymerization of MMA, leaving several possibilities open for attachment of the growing polymer (PMMA) on the poly(DCPD) backbone [129].

The spectrum of the bleed revealed that a polymer blend was obtained after self-healing. In this spectrum, the bands from PMMA were assigned to the C=O stretch at 1731 cm^{-1} and

the C–O stretches in the 1140–1250 cm^{-1} region. ROMP polymers can display different characteristics, such as *cis/trans* isomerization, tacticity, *etc*. In the spectrum of the bleed, the signal at 966 cm^{-1} was assigned to the carbon hydrogen bending vibration of a trans carbon double bond of the ring-opened poly(DCPD) [57, 112, 130,131]. This signal interfered with the band at 987 cm^{-1} and shoulder at 966 cm^{-1} that belong to the O–CH$_3$ b

ending and C–CH$_3$ rocking in PMMA.
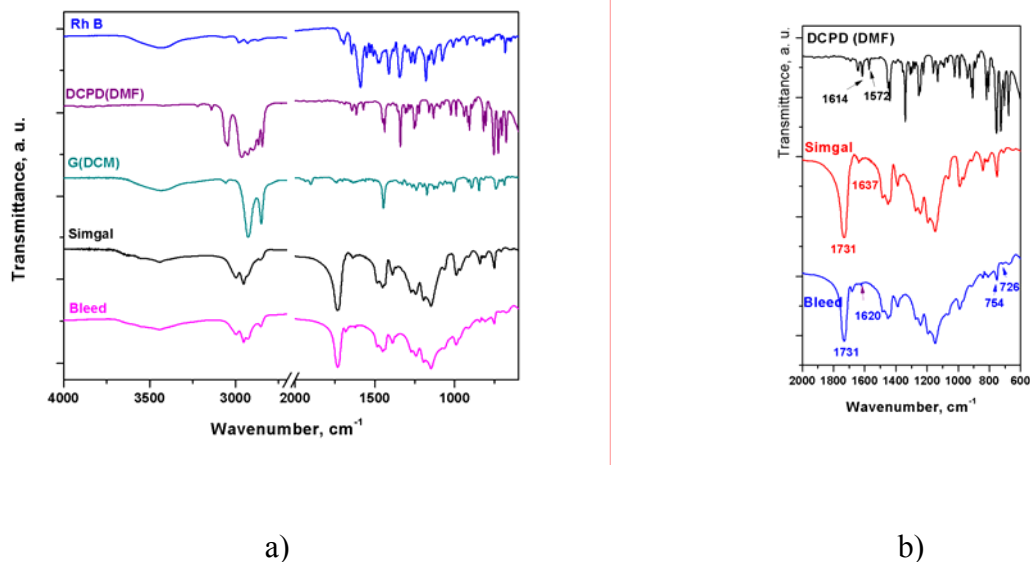
Figure. 34. FTIR spectrum of starting materials and the self-healing bleed: a) RhB-Rhodamine B; DCPD (DMF) - 10 wt. % DCPD solution in DMF; G (DCM) - 1 wt. % Grubbs' solution in DCM; poly(DCPD) (RhB) - ROMP polymer DCPD with RhB; (b). Spectrum of DCPD (DMF), Simgal and the bleed [77]

Morphology of SH composites

The micrograf of crack after impact and FESEM of fracture of SH sample are presented on Figure 40. From the micrograph could be seen how the self healing process start (Fig 40a) and how the SH bleed was formed.
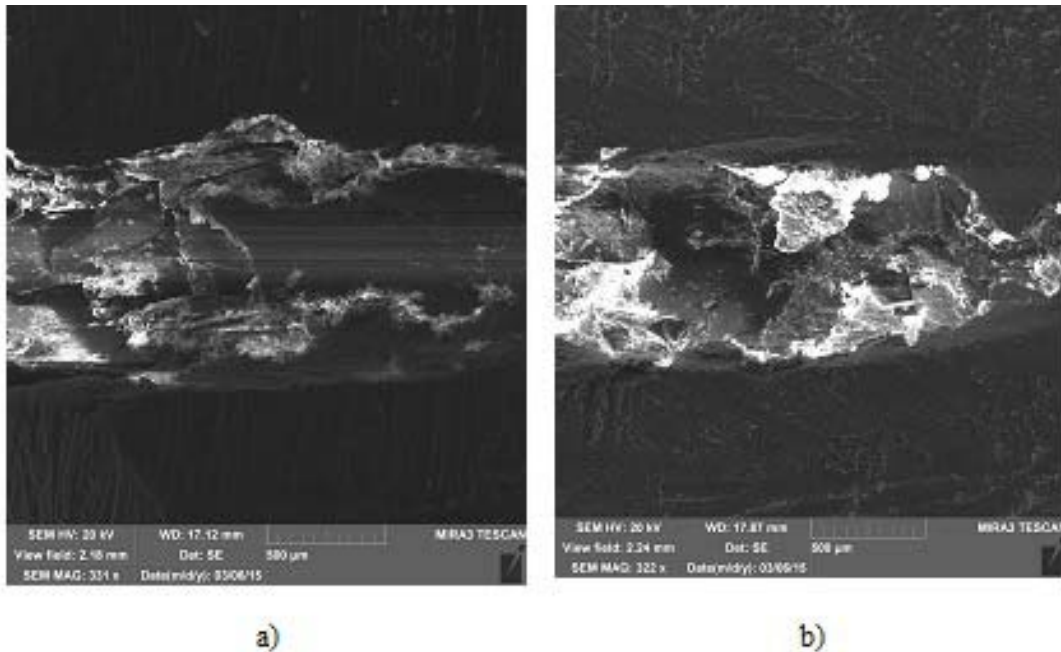

Figure 35. The FESEM of SH fracture a) The fractrure of glass tube; b) The formed SH bleed

DSC of SH Composites

DSC analysis of Simgal and SH bleed (the second scans) are presented in Fig. 36. The glass transition temperature T_g of Simgal as an auto polymerized denture base polymer was considerably lowered because of the residual MMA content – 85 °C [56, 57]. Among the properties that could be affected by the presence of residual monomers in the acrylic resin is its T_g, due to the plasticizing effect of the MMA. In addition, it was observed that cross linked polymers are less flexible and have a much higher T_g than the corresponding non-cross linked or partially cross linked polymers. Therefore, the low T_g demonstrated by Simgal could be attributed to the presence of residual monomers in its composition. From

the scan for the SH bleed, a T_g of 37 °C was determined for poly(DCPD), which indicated that it was not fully cured, because the T_g of fully cured poly DCPD is 139 ºC [132]. The exothermic curing peak obtained on the DSC scan for SH bleed. This peak can tell us that second step of polymerization is not complete and after additional heating of the pDCPD, more crosslinking between polymer chains can be created [133-136].

The catalyst concentration had a large effect on the cure kinetics and this curing could be followed by DSC. The position of the exothermic curing peak revealed the ROMP polymerization (Fig. 1) and corresponded to the temperature range for low to medium concentrations of catalyst, as was stated by Kessler and White [133]. The missing T_g onset point in the region 80–85 °C indicated that residual MMA monomer was consumed. In addition, it was suggested that the presence of RhB [16] in the SH bleed also shifted the T_g of pure polymerized acrylic resin to higher temperatures and was superposed with the exothermic cured peak. This result, which implies further polymerization of MMA, is in agreement with the FTIR analysis, which also revealed bands assigned to poly(DCPD) and PMMA.
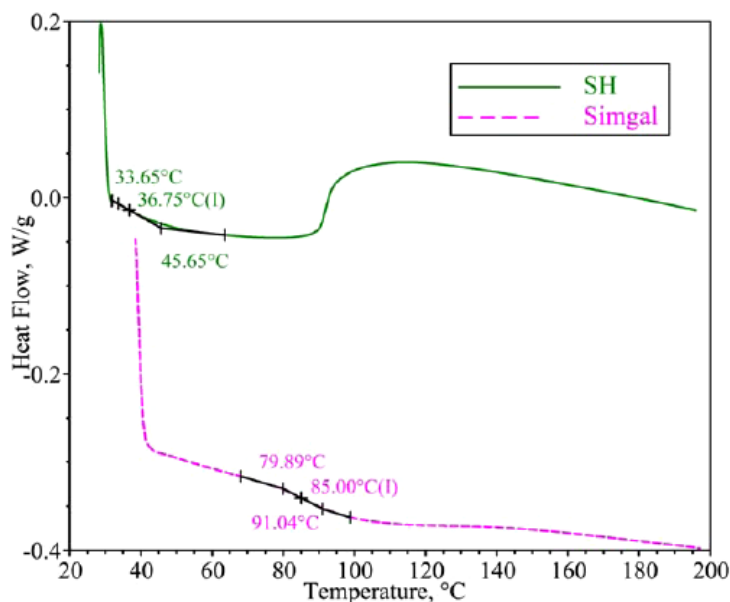

**Figure. 36. DSC analysis of Simgal and SH bleed, second scan [77]**

Umpact test of SH Composite

The image of the sample surface immediately after the impact test is presented in Fig. 37 and the start of leaking of liquid SHA could be seen. It could also be seen that the rose-colored liquid SHA was released from the fracture. The image of the same sample and the healed surface 96 h after the first impact test is presented in Fig. 38. The violet self-healed bleed - the cured (polymerized) poly(DCPD) - is visible.


**Figure 37. The sample immediately after the impact test (with the liquid SHA on the surface) [77]**
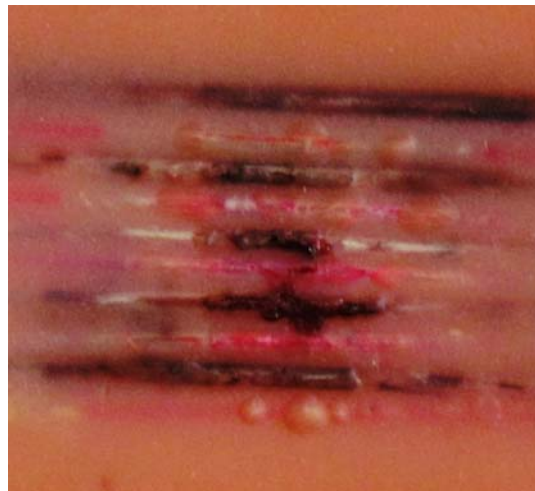
Figure 38. The sample 96 h after the first impact test (with the cured polymer on the surface) [77]

The results of impact tests are presented in Figures 39 and 40. The load-time diagram is presented in Fig. 39 for samples of all three series: the original (0), the control with empty tubes (ET) and virgin with SHA filled tubes (SH 1). According to the shapes of the curves [137], the failure mode of the specimens was changed from ductile for the original sample, to ductile/brittle failure for the samples with tubes (Fig. 39).
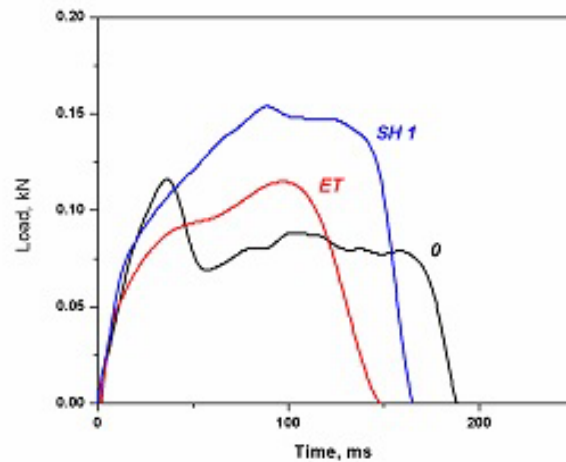
Figure 39. The load-time curves for the original sample (0), the control sample with empty tubes (ET) and the virgin sample with SHA filled tubes (SH 1) [77]

Load-time curves for the evaluation of the self healing effect are presented in Fig. 40. It is obvious that the curve for SH_{healed} followed the shape of the virgin sample and the load peak was at 87 % of the value for SH_{virgin}. The results of impact test relative to load and energies are presented in Table 7. According to the peak value of the load, the self-healing efficiency η was 87 %; for the energy to load peak, η was 83 % and 81 % for the total energy.
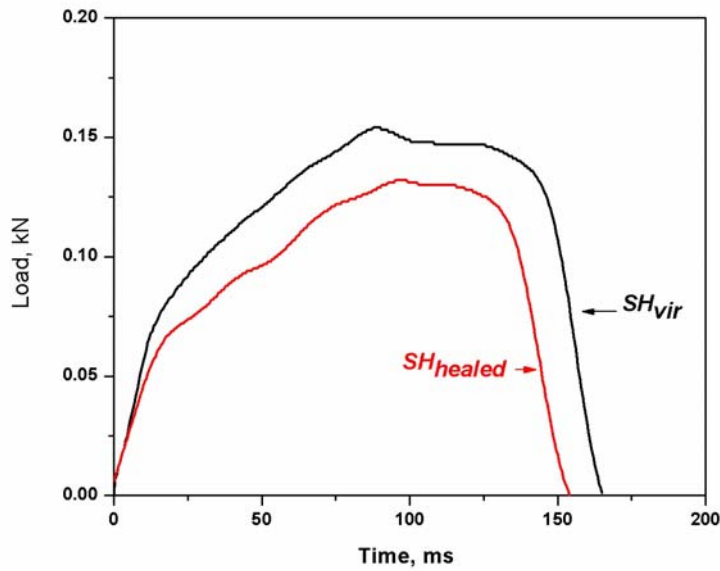
Figure 40. The load-time curves for virgin (SH$_{virgin}$) and healed (SH$_{healed}$) samples with SHA [77]

The slope of the linear part of the load – displacement curve is proportional to the modulus of elasticity [138]. The slope for healed sample was 80 % of the value of the virgin sample. These results revealed that the self-healing system of filling tubes with a solution of SHA was successfully applied to acryl ate.

Table 7. Load, energy to load peak and total energy healing efficiency

Sample	SH $_{virgin}$	SH $_{healed}$	η , %
Load peak, kN	0.15	0.13	87
Energy to load peak, J	0.24	0.20	83
Total energy, J	0.27	0.22	81
Slope, kN/mm	0.05	0.04	80

Nanoindentation of SH composite

The results of the nanoindentation test are presented in Table 8 and Fig. 41. The load–depth plots of indentations on the surface of the same sample fabricated with SHA tubes are presented in Fig. 40a.
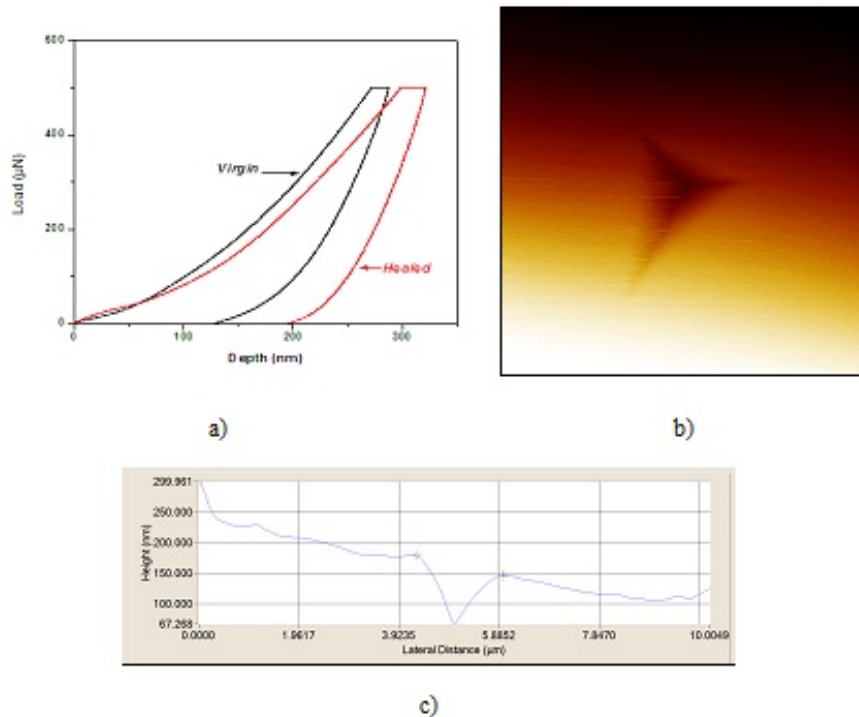
Figure 41. a) Load–displacement curves of a virgin and a healed surface; b) indent on virgin sample; c) scan trace of the sample [77]

The curves appear to be with continuity and without pop in or pop out in both loading and unloading phases. The average maximum depth of the peak load from the virgin surface was approximately 287 nm, while for the healed sample, it was 320 nm. The results of

reduced elastic modulus and hardness of the virgin and healed surfaces are presented in Table 4, and they are in accordance with literature data [139-142].

Table 8. *Results of the nanoindentation test*

Surface	E_r (MPa)	Standard deviation, GPa	H, (GPa)	Standard deviation, GPa
Virgin	4.895	± 0.23	0.331	± 0.020
Healed	3.849	± 0.16	0.247	± 0.015

The reduced modulus and hardness for the healed surface was about 79 % and 75 % in comparison to the virgin surface, respectively.

Conclusion

In this dissertation the posibility of synthesis of composites with improoved mechanical, thermal properties and functionality of composite materials with polymer matrix for use in dentistry was investigated. Synthesis and characterisation of nano to mikro modified dental composites on the basis of autopolymerized acrylates are performed.

The composite acrylic resin with embedded unmodified alumina whiskers, silanized alumina whiskers, Zeolite and self-healing agents was processed and characterized. The content of whiskers was 3% w/w. The modification of the nano whiskers with the MPTMS silane enabled their dispersion and deagglomeration and yielded enhanced mechanical properties of the composite materials. The DSC results revealed that the glass transition (T_g) of the acrylic resin with silanized whiskers was greater than those of pure acrylic resin and resin with unmodified whiskers. As shown by nanoindentation tests, incorporation of 3 % w/w of silanized nano whiskers increased the reduced modulus and hardness of acrylic resin composite for 65% and 90%, respectively. The nanowhiskers behaved as crosslinking agent and inhibited the motion of molecular chains. Moreover, the enhanced interface bonding between matrix and whiskers via hydrogen bonds realized better stress distribution during loading.

Also, the composites with different content of Zeolite particles were processed and characterized. The influence of zeolite content on the mechanical and thermal properties of the composites was studied. DSC results revealed that zeolite does not significantly affect Tg acrylic and is slightly lower. Test results of impact test revealed that embedding of zeolite increases the absorbed energy. These results indicate that the addition of Zeolite improved mechanical properties of acrylic resin. In addition, its structure allows functionalization of composites. Further research into the introduction of Zeolite in acrylate in the dental care should be taken in the direction of functional ion compounds and precursors that can be incorporated into the zeolite and that the grid would further controlled release, and functionally improved composite.

In this study, the processing and characterization of acrylic resin and an evaluation of self-healing properties were realized. To the best of our knowledge, solutions of DCPD and Grubbs' catalyst were not hitherto used for filling tubes embedded in thermoplastic acrylic resin. The use of a solution of DCPD in DMF and Grubbs' of the first generation in DCM gave a dental acrylic resin with new properties. FTIR analysis revealed ROMP polymerized poly(DCPD) in the healed bleed and formation of polymer blend. DSC analysis also revealed the further polymerization of acrylic resin and a poly (DCPD) with Grubbs' as the tandem catalyst. This reaction decreased the content of residual monomer in thermoplastic acrylic resin and could prevent emission of residual monomer out of the sample. The investigation of impact behavior revealed the load peak self-healing efficiency of 87 %; and for energy to load peak and to total energy were 83 % and 81 %, respectively. According the nanoindentation test on virgin and healed surfaces, restoration of the reduced modulus of elasticity and hardness were obtained by self-healing.

References:

1. F.C. Campbell, Structural Composite Materials, Copyright © ASM International, 2010

2. L.H. Sperling Introduction to physical polymer science, fourth edition John Wiley & Sons, Inc.,. Hoboken, New Jersey, 2006.

3. B. Wunderlich, Macromolecular Physics, Academic Press, Inc. New York, 1973

4. W. D. Callister, Materials Science and Engineering, An Introduction, John Wiley & Sons, Inc., 2007

5. Bryan Harris, Engineering Composite Materials, The Institute of Materials, London, 1999

6. Polymer Composites: Volume 1, First Edition. Edited by Sabu Thomas, Kuruvilla Joseph, Sant Kumar Malhotra, Koichi Goda, and Meyyarappallil Sadasivan Sreekala, Wiley-VCH Verlag GmbH & Co. KGaA. Published 2012 by Wiley-VCH Verlag GmbH & Co. KGaA2012

7. I. A. Mjor, C. Shen, S.T. Eliasson, S. Richter, *Oper Dent*, (2002), 27, 117.

8. I. A. Mjor, *Acta Ordont. Scand.* (1997), 55, 53.

9. B. Fissore, J. Nicholls, R. Yuodelis, *J Prosthet Dent* (1991), 65,80.

10. G. J. Christensen, *The Journal of the American Dental Association*, (1999), 130,2, 275

11. E.A. Ayaz, and R. Durkan, *Int. J. Oral Sci*., (2013) 5, 229.

12. R. Gautam, R.D. Singh, V.P. Sharma, R. Siddhartha, P. Chand, R. Kumar, *J. Biomed. Mater. Res. Part B*, (2012), 100, 1444.

13. P.H.H. Arajo, C. Sayer, R. Giudici, and J.G.R. Poo, *Polym. Eng. Sci.*, (2002)42, 442.

14. R.S. Seo, H. Murata, G. Hong, C.E. Vergani, and T. Hamada, *J. Prost. Dent*., (2006), 96, 59.

15. M. Braden, *Adv. Dent. Res.*, (1988), 2, 93.

16. R. M. Dukali, I. M. Radovic, D. B. Stojanovic, D. M. Sevic, V. J. Radojevic, D. M. Jocic, R. R. Aleksic, *J. Serb. Chem. Soc.* (2014),79, 7.

17. J.H. Jorge, E.T. Giampaolo, A.L. Machado, A.C. Pavarina, I.Z. Carlos, *Gerodontology* (2007), 24(1):52-57.

18. R. Q. Frazer, R.T. Byron, P.B. Osborne, K.P West. *J. Long Term Eff. Med. Implants* (2005), 15, 6, 629.

19. AT.H. Tang , J. Li , J Ekstrand , Y. Liu .,*Int Biomed Mater Res.* (1999) 45, 214.

20. I. Teraoka, Polymer solutions: an introduction to physical properties, John Wiley & Sons, Inc., New York, 2002

21. Drummond JL. *Journal of Dental Research*, (2008), 87, 8, 710-719.

22. C Santos, RL Clarke, M Braden, F Guitian, KWM Davy, *Biomaterials,* (2002), 23, 8, 1897.

23. E. Ellakwa, M. A. Morsy, Ali M. El-Sheikh, *J. of Prosthodon*. 17 (2008) 439.

24. C. Mugoni, A. Licciulli, D. Diso, C. Siligardi, *Ceram. Inter.* 41 (2015), 13090–.

25. H. H. K. Xu, F. C. Eichmiller, J. M. Antonucci, G.E. Schumacher, L.K. Ives, *Dent. Mater.* 16 (2000) 356.

26. Ruddle DE, Maloney MM, Thompson IY. *Dent. Mater.* 18(1) (2002) 72.

27. H. H. K Xu, G. E. Schumacher, F. C. Eichmiller, R. C. Peterson, J. M. Antonucci, H. J. Mueller, *Dent. Mater.* 19(6) (2003) 523.

28. D.R/ Burns, D.A. Beck, S.K. Nelson, *J. Prosthet. Dent*. 90 (2003) 474.

29. J Manhart, KH Kunzelmann, HY Chen, R Hickel . *Journal of Biomedical Materials Research*, (2000) 53, 4353.

30. Y. Papadogiannis, R. Lakes , G. Palaghias, M. Helvatjoglu-Antoniades, D. Papadogiannis, *Dental Materials,* (2007), 23, 2, 235.

31. Y. Li, ML Swartz, RW Phillips, BK Moore, TA Roberts. *Journal of Dental Research* (1985), 64, 12, 1396.

32. G. Meric, JE Dahl, IE Ruyter, *European Journal of Oral Sciences*, (2005), 113, 3, 258.

33. JWV Van Dijken, K. Sunnegardh-Gronberg. *Journal of Dentistry*, (2006), 34, 10, 763.

34. MA Freilich , JC Meiers, JP Duncan J. Fiber-reinforced composites in clinical dentistry. 2000. First edition, Quintessence Publishing.

35. Xu HHK. *Journal of Dental Research*, (2003), 82, 1, 48.

36. J. C. J. Webb, R. F. Spencer, *J. Bone Joint. Surg.* 89-B (2007) 851.

37. S. A. Ben Hasan, M. M. Dimitrijević, A. Kojović, D. B. Stojanović, K. Obradović-Đuričić, R. M. Jančić Heinemann and R. Aleksić, *J. Serb. Chem. Soc. 79* (10) (2014) 1295.

38. F. A. Alzarrug, M. M. Dimitrijević, R. M. Jančić Heinemann, V. Radojević, D. B. Stojanović, P. S. Uskoković, R. Aleksić, *Mater. Design.* 86 (2015) 575.

39. J. Alvarado-Rivera, J. Muñoz-Saldaña, A. Castro-Beltrán, J. M. Quintero-Armenta, J. L. Almaral-Sánchez, and R. Ramírez-Bon, *Phys. Stat. Sol.* (2007) 4, 11, 4254.

40. R.L/ Price, L.G. Gutwein, L. Kaledin, F.Tepper, T.J. Webster, *J Biomed Mater Res A.* (2003), 67, 4,1284.

41. Dental Materials and Their Selection- 3rd Ed William J. O'Brien. Quintessence Publishing Co, Inc. Chicago, 2002

42. Wallenberger FT and Brown SD, *Compos Sci & Tech,* (1994), 51, 243.

43. P. Singh, N. Kumar, R. Singh, K. Kiran, S. Kumar, *International Journal of Scientific Study*, (2015), 3, 9, 169.

44. Yeli M, Kidiyoor KH, Nain B, Kumar P. *J Oral Res Rev* (2010), 2, 8.

45. JL Joyee, CN Cook. *Dent Clin Update* (2003), 25, 19-21.

46. Cohen R. *Dent Town,* (2008), 64, 25-35.

47. N Attar, LE Tam, D McComb, *J Can Dent Assoc,* (2003), 69, 516.

48. S.Nandini *J Conserv Dent* 2010;13:184.

49. Beyth N, Yudovin-Farber I, Bahir R, Domb AJ, Weiss EI. *Biomaterials*, (2006) 27, 3995.

50. SF Rosensteil, MF Land, J. Fujimoto Contemporary Fixed Prosthodontics. 3rd ed. St. Louis: Mosby; 2001. p. 697.

51. MA Freilich, JC Meiers, JP Duncan, AJ Goldberg. Fibrereinforced Composite in Clinical Dentistry. Chicago: Quintessence Publishing Co.,Inc.; 2000.

52. V. Badami, B.Ahuja, *Scientific World Journal* (2014), 2014:986912.

53. IE Yuzay, R Auras, S. Selke, *J Appl Polym Sci,* (2010), 115, 2262.

54. A. Yuzay, E.Isinay, R. Auras, H. Soto-Valdez, S. S. Selke, *Polym. Degrad. Stabil.* (2010), 95, 1769.

55. A. Satya , S. Subramanian, R. Seeram, *Journal of Inorganic Materials*, (2012), 27, 3, 332

56. Y. C. Yuan, T. Yin, M. Z. Rong, and M. Q. Zhang, *Express Polym. Lett.*, (2008), **2**, 238.

57. S.R. White, N.R. Sottos, P.H. Geubelle, J.S. Moore, M.R. Kessler, S.R. Sriram, E.N. Brown, and S. Viswanathan, *Nature*, (2001), 409, 794.

58. G.E. Larin, N. Bernklau, M.R. Kessler, and J.C. Di Cesare, *Polym. Eng. Sci.,* (2006), 46, 1804.

59. L. Guadagno, M. Raimondo, C. Naddeo, P. Longo, A. Mariconda, *Polym. Eng. Sci.,* (2014), 54, 777.

60. M. Raimondo, and L. Guadagno, *Polym. Compos*, (2013), 1525.

61. M.R. Kessler, N.R. Sottos, and S. R. White, *Composites Part A*, 34, (2003)743.

62. R.S.Trask, H.R.Williams, and I. P. Bond, *Bioinspir. Biomim*, (2007), 12, 1.

63. A.J. Patel, N.R. Sottos, E.D. Wetzel, and S.R. White, *Composites Part A*, (2010), 41, 360.

64. E.B. Murphy, and F. Wudl, *Prog. Polym. Sci.*, (2010), 35, 223.

65. T. Gumula, and P. Szatkowski, *Polym. Compos*, 1 (2014), DOI: 10.1002/pc.23287.

66. S. Bleay, C. Loader, V. Hawyes, L. Humberstone, and P. Curtis, *Composites Part A,* (2001), 32, 1767.

67. J.W.C. Pang, and I.P. Bond, *Compos. Sci. Technol.*, (2005), 65, 1791.

68. J.W.C. Pang, and I.P. Bond, *Composites Part A*, (2005), 36, 183.

69. R.S. Trask, and I.P. Bond, *Smart Mater. Struct.*, (2006),15, 704.

70. G. Williams, *Composites Part A,* (2007), 38, 1525.

71. R.S. Trask, G.J, Williams, and I.P. Bond, *J. R. Soc. Interface,* (2007), 4, 363.

72. K.S. Toohey, N.R. Sottos, J.A. Lewis, J.S. Moore, S.R.White, *Nat. Mat.*, (2007), 6, 581.

73. D. Therriault, R.F. Shepherd, S.R White, J.A. Lewis, *Adv. Mat.*, (2005), 17, 394.

74. X. Ouyang, X. Huang, Q. Pan, C. Zuo, C. Huang, X. Yang, and Y. Zhao, *J. Dent.*, (2011), 39, 825.

75. B.E. Wertzberger, J.T. Steere, R.M. Pfeifer, M.A. Nensel, M.A. Latta, S.M. Gross, *J. Appl. Polym. Sci.*, (2010), 118, 428.

76. S. Then, G.S. Neon, and N.H. Abu Kasim, *J. Appl. Polym. Sci.*, (2011), 122, 2557.

77. O.Yerro, V. Radojević, I. Radović, M. Petrović, P.Uskoković, D.Stojanović, R. Aleksić, Thermoplastic acrylic resin with self-healing properties, *Polymer Engineering and Science*, (2016), 56, 3,251.

78. J.M/ Antonucci, S.H/ Dickens, B.O. Fowler, HHK Xu, W.G.McDonough, *Journal of Research of the National Institute of Standards and Technology,* (2005), 110, 5, 541.

79. J. Eick, S. Kotha, C. Chappelow, K. Kilway, G. Giese, A. Glaros, C. Pinzino, *Dental Materials*, (2007), 23, 8, 1011.

80. K. Sato, A.Ijuin,Y. Hotta, *Ceram. Inter.* (2015), 41, 10314

81. J. P. Matinlinna, V.J. L. Lassila, P. K. Vallittu, *Dental materials* 23 (2007), 1173

82. G. Mohammadnezhad, M. Dinari, R. Soltani, Z. Bozorgmehr, *Appl. Surf. Sci.* 346 (2015) 182.

83. O. Yerro, V. Radojević, I. Radović, A. Kojović, P. S. Uskoković, D. B. Stojanović, R. Aleksić, *Ceram. Inter.*, (2016), 42, 9, 10779.

84. D. Stojanovic, A. Orlovic, S. Markovic, V. Radmilovic, Petar S. Uskokovic, R. Aleksic, *J. Mater. Sci.* (2009), 44, 23, 6223.

85. M. Pires, M. Murairu, P*roceedings of the 3rd International Conference on Maritime and Naval Science and Engineering,* 45-50. Constantza, Romania , 2010

86. D.B. Stojanović, M. Zrilić, R. Jančić-Heinemann, I. Živković, A. Kojović, P.S. Uskoković, R. Aleksić, *Polym Adv Technol*, (2013), 24, 772.

87. N.V. Padaki, R. Alagirusamy, B.L. Deopura. *Indian J Fiber Text,* (2008), 33, 189.

88. V.Obradović, D.B.Stojanović, I. Živković, V. Radojević**,** P.S.Uskoković, R. Aleksić, *Fibers and Polymers,* (2015), 16, 1, 138.

89. C. Oliver, G.M. Pharr, *J. Mater. Res*. 7 (1992) 1564.

90. ISO/CD 14577 - 1, 2 & 3 : Metallic materials - Instrumented indentation test for hardness and other material properties, (1999),

91. D. Yang, B. Paul, W. Xu, Y. Yuan, E. Liu, X. Ke, R.M. Wellard, C.Guo, Y. Xu, Y.Sun, H. Zhu, *Water Res*. 44 (2010) 741.

92. M.M. Caruso, D.A. Delafuente, V. Ho, N.R. Sottos, J.S. Moore, S.R. White, *Macromolecules*, (2007) 40, 8830.

93. D. Yang, B. Paul, W. Xu, Y. Yuan, E. Liu, X. Ke, R.M. Wellard, C.Guo, Y. Xu, Y.Sun, H. Zhu, *Water Res.* (2010), 44, 741.

94. I. L.Lagadic, M. K. Mitchell, B. D.Payne, *Environ. Sci. Technol.* (2001), 35 984.

95. L. G. Bach, Md. R. Islam, Y. T. Jeong, H. S. Hwang, K. T. Lim, *Mol. Cryst. Liq. Cryst.* 565 (2012) 78–87.

96. M. Hu, S. Noda, T. Okubo, Y. Yamaguchi, H. Komiyama, *Appl. Surf. Sci.* 181 (2001) 307.

97. V. C. Farmer, The Infrared Spectra of Minerals. Mineralogical Society, London, 1974

98. J. A. Gadsden, Infrared Spectra of Minerals and Related Inorganic Compounds, 1975, London.

99. X. Zhang, X. Zhang, B.Zhu, K. Lin, J. Chang, *Dent. Mater*. (2012) 31, 6, 903.

100. D.R. Burns, D.A. Beck, S.K. Nelson, *J. Prosthet. Dent.* (2003) 90, 474.

101. M. Kostic, N. Krunic, L. Nikolic, V. Nikolic, S. Najman, and J. Kocic, *Vojnosanit. Pregl.* (2009), 66, 223.

102. C .B. Roth, J. R. Dutcher, *Eur. Phys. J. E.* (2003), 12, 91.

103. M. Vacatello, *Macromolecules,* (2001), 34, 6, 1946.

104. P. Thomas, B. S. Dakshayini, H. S. Kushwaha, R. Vaish, *J. Adv. Dielect.* (2015), 5, 2, 1550018 (11 pages) DOI: 10.1142/S2010135X15500186

105. B. J. Ash, R. W. Siegel, L. S. Schadler, *J. Polym. Sci. Part B, Polym. Phys.* (2004), 42, 23, 4371.

106. K. D. Jandta, B. W. Sigusch, , *Dent. Mat.* (2009), 25, 1001.

107. J. Alvarado-Rivera, J. Muñoz-Saldaña and R. Ramírez-Bon   Elastic and Nanowearing Properties of SiO$_2$-PMMA and Hybrid Coatings Evaluated by Atomic Force Acoustic Microscopy and Nanoindentation", Scanning Probe Microscopy-Physical Property Characterization at Nanoscale, Dr. Vijay Nalladega (Ed.),.ISBN: 978-953-51-0576-3, InTech, Croatia, 2012

108. Sanchez-Soto M., Martınez A. B., O. O.Santana, A.Gordillo, *J. Appl. Polym. Sci.* (2004), 93, 1271.

109. A. Majumdar, B. S. Butola, *Mater. Design.* (2013), 51, 148.

110. D. Schaubroeck, S. Brughmans, C. Vercaemst, J. Schaubroeck, F. Verpoort, *J. Mol. Catal. A-Chem.* (2006), 254, 180.

111. S.E. Barnes, E.C. Brown, N. Corrigan, P.D. Coates, E. Harkin-Jones, H.G.M. Edwards, *Spectrochim. Acta, Part A.*, (2005), 61, 2946.

112. G.S.Constable, A.J. Lesser, and B. Coughlin, *J. Polym. Sci. B.*, (2003), 41, 1323.

113. B.J. Rohde, M. L. Robertson, and R. Krishnamoorti, *Polymer*, (2015), 69, 204.

114. I.S. Elashmawi, and N.A. Hakeem, *Polym. Eng. Sci.*, (2008), 48, 895.

115. F. Goldibi, and G. Asghari, *Res. J. Biol. Sci.*, (2009), 4, 244.

116. N. Celebi, B. Yuzugullu, S. Canay, and U. Yucel, *Polym. Adv. Technol.*, (2008),19, 201.

117. F. Bettencourt, C.B. Neves, M.S. De Almeida, L.M. Pinheiro, S. Arantes e Oliveir, L.P. Lopes, and F.M. Castr, *Dent. Mat.*, (2010), 26, 171.

118. J.A. Bartoloni, D.F. Murchison, D.T. Wofford, N. Sarkar, *J. Oral Rehabil.*, (2000), 27, 488.

119. M.J. Azzari, M.S. Cortizo, and J.L. Alessandrini, *J. Dent.*, (2003), 31, 463.

120. S.Y. Lee, Y.L. Lai, and T.S. Hsu, *Eur. J. Oral Sci.*, (2002), 110, 179.

121. C.W. Bielawski, J. Louie, and R.H. Grubbs, *J. Am. Chem. Soc.*, (2000),122, 12872.

122. C. Cheng, E. Khoshdel, and K.L. Wooley, *Nano Lett.*, (2006), 6, 1741.

123. J.S.Wang, and K. Matyjaszewski, *Macromolecules*, 28, (1995), 7572.

124. J. Gromada, and K. Matyjaszewski, *Macromolecules*, (2001), 34, 7664.

125. W. Jakubowski, and K. Matyjaszewski, *Macromolecules*, (2005), 38, 4139.

126. W. Jakubowski, K. Min, and K. Matyjaszewski, *Macromolecules*, (2006), 39, 39.

127. K. Matyjaszewski, W. Jakubowski, K. Min, W. Tang, J. Huang, W.A. Braunecker, and N.V. Tsarevsky, *PNAS*, (2006), 103, 15309.

128. C.J. Fristrup, K. Jankova, and S. Hvilsted, *Soft Matter*, (2009), 5, 4623.

129. D.P. Mohite, S. Mahadik-Khanolkar, H. Luo, H. Lu, C. Sotiriou-Leventis, N. Leventis, *Soft Matter*, (2013), 9, 1516.

130. L. Guadagno, and M. Raimondo, Use of FTIR Analysis to Control the Self-Healing Functionality of Epoxy Resins in Infrared Spectroscopy Materials Science, Engineering and Technology, InTech 2012.

131. S.T. Nguyen, L.K. Johnson, and R.H. Grubbs, *J. Am. Chem. Soc.*, (1992), 114, 3974.

132. M.R. Kessler, and S.R. White, *J. Polym. Sci., Part A: Polym. Chem.*, (2002), 40, 2373.

133. D.A. Rusakov, A.A. Lyapkov, E.I. Korotkova, N.V. Thanha, T.Q. Cuonga, and M.K. Zamanova, *Procedia Chemistry,* (2014), 10, 490.

134. G. H. Hsiue, H. F. Wei, S. J. Shiao, W. J. Kuo, Yi-An Sha, *Polymer Degradation and Stability,* (2001), 73, 309

135. D. P. Mohite, S. M. Khanolkar , H. Luo , H. Lu, C. S. Leventis, N. Leventis, *Soft Matter,* (2013), 9, 1516

136. M. J. Abadie, M. Dimonie, C. Couve, V. Dragutan, *European Polymer Journal,* (2000), 36, 1213

137. V. Shah, Handbook of plastics testing and failure analysis, John Wiley & Sons, New Jersey, 2007

138. D.E. Mouzakis T. Harmia, and J. Karger-Kocsis, *Polym. Compos.*, (2000), 8, 167.

139. S. Balos, B. Pilic, D. Markovic, J. Pavlicevic, and O. Luzanin, *J. Prosthet. Dent.*, (2014), 111, 327.

140. S. J. Vivanco, D. Ebenstein, M. Squire, H. L. Ploeg, *J. Mech. Behav. Biomed.* (2014), 37, 141.

141. L. Perea, J. P. Matinlinna, M. Tolvanen, L. V. Lassila, P. K. Vallittu, *J. Prosthet. Dent.*, (2014),112, 257.

142. M. J. F. Bindo, A. E. M. Nakamae, L. de Brito Santos, K. H. Ishikawa, T. de Carvalho Guarnieri, and R. Tamaki, *Braz. Oral Res.,* (2009), 23, 68.

Biography

Omer Mohamed Yerro was born 30.07.1983. in Nalut, Libya. He is attended High school hje in Nalut and graduated 2000. He graduated 2005. on Faculty of medical Technology on University EL-Jabel EL-Garbi. The Master Degree he finished 2011. in University of Belgrade, Faculty of Technology and Metallurgy, Department of Materials Engineering. He is enrolled in PhD studies from 2012. at University of Belgrade, Faculty of Technology and Metallurgy, Department of Materials Engineering.

He was employed as assisted researcher in Department of Dental Technology in Faculty of medical Technology on University EL-Jabel EL-Garbi until 2005.

Biografija

Omer Mohamed Yerro rođen je 30.07.1983. u Nalutu, Libija. Srednju školu je završio u Nalutu 2000. godine. Diplomirao je 2005. na Fakultetu medicinske tehnologije na Univerzitetu EL-Jabel EL-Garbi. Master studije je završio 2011. na Univerzitetu u Beogradu, Tehnološko-metalurški fakultet, profil Inženjerstvo materijala. Doktorske studije na Univerzitetu u Beogradu, Tehnološko-metalurški fakultet, profil Inženjerstvo materijala upisao je 2012 godine.

Od 2005. godine zaposlen je na Fakultetu medicinske tehnologije na Univerzitetu EL-Jabel EL-Garb kao asistent na odseku Dentalne tehnologije.

Appendix 1

Appendix 2

Прилог 2.

Изјава о истоветности штампане и електронске верзије докторског рада

Име и презиме аутора ___ Omer Mohamed Yerro ___

Број индекса ___ 4070/2011 ___

Студијски програм ___ Инжењерство Материјала ___

Наслов рада ___ Sinteza i karakterizacija funkcionalnih kompozitnih materijala za primenu u stomatologiji ___

Synthesis and characterization of functional composite materials for applications in dentistry

Ментор ___ Радојевић Весна ___

Потписани/а ___

Изјављујем да је штампана верзија мог докторског рада истоветна електронској верзији коју сам предао/ла за објављивање на порталу **Дигиталног репозиторијума Универзитета у Београду.**

Дозвољавам да се објаве моји лични подаци везани за добијање академског звања доктора наука, као што су име и презиме, година и место рођења и датум одбране рада.

Ови лични подаци могу се објавити на мрежним страницама дигиталне библиотеке, у електронском каталогу и у публикацијама Универзитета у Београду.

Потпис докторанда

У Београду, ___ 04. 04. 2016. ___

Appendix 3

1. Ауторство - Дозвољавате умножавање, дистрибуцију и јавно саопштавање дела, и прераде, ако се наведе име аутора на начин одређен од стране аутора или даваоца лиценце, чак и у комерцијалне сврхе. Ово је најслободнија од свих лиценци.

2. Ауторство – некомерцијално. Дозвољавате умножавање, дистрибуцију и јавно саопштавање дела, и прераде, ако се наведе име аутора на начин одређен од стране аутора или даваоца лиценце. Ова лиценца не дозвољава комерцијалну употребу дела.

3. Ауторство - некомерцијално – без прераде. Дозвољавате умножавање, дистрибуцију и јавно саопштавање дела, без промена, преобликовања или употребе дела у свом делу, ако се наведе име аутора на начин одређен од стране аутора или даваоца лиценце. Ова лиценца не дозвољава комерцијалну употребу дела. У односу на све остале лиценце, овом лиценцом се ограничава највећи обим права коришћења дела.

4. Ауторство - некомерцијално – делити под истим условима. Дозвољавате умножавање, дистрибуцију и јавно саопштавање дела, и прераде, ако се наведе име аутора на начин одређен од стране аутора или даваоца лиценце и ако се прерада дистрибуира под истом или сличном лиценцом. Ова лиценца не дозвољава комерцијалну употребу дела и прерада.

5. Ауторство – без прераде. Дозвољавате умножавање, дистрибуцију и јавно саопштавање дела, без промена, преобликовања или употребе дела у свом делу, ако се наведе име аутора на начин одређен од стране аутора или даваоца лиценце. Ова лиценца дозвољава комерцијалну употребу дела.

6. Ауторство - делити под истим условима. Дозвољавате умножавање, дистрибуцију и јавно саопштавање дела, и прераде, ако се наведе име аутора на начин одређен од стране аутора или даваоца лиценце и ако се прерада дистрибуира под истом или сличном лиценцом. Ова лиценца дозвољава комерцијалну употребу дела и прерада. Слична је софтверским лиценцама, односно лиценцама отвореног кода.